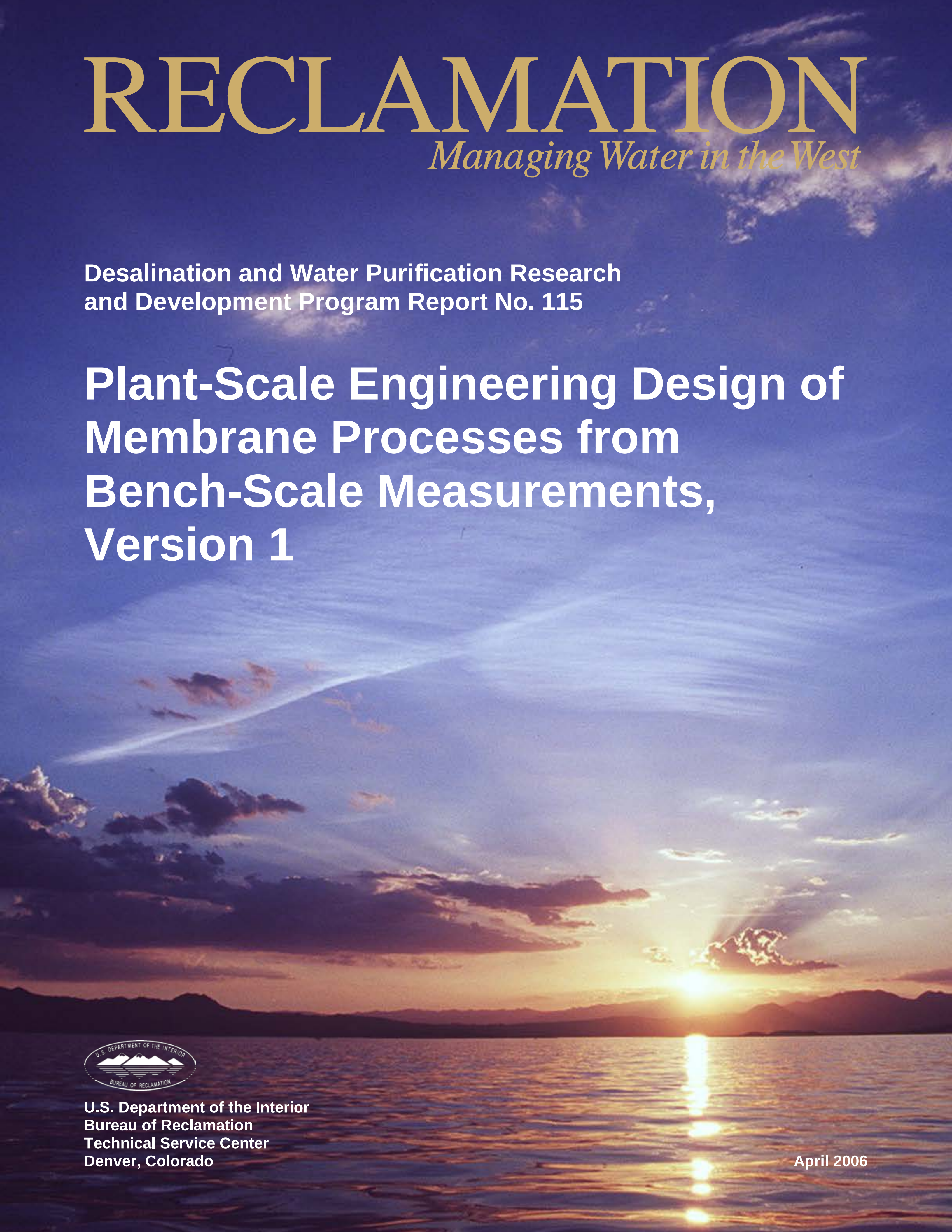

RECLAMATION

Managing Water in the West

Desalination and Water Purification Research
and Development Program Report No. 115

Plant-Scale Engineering Design of Membrane Processes from Bench-Scale Measurements, Version 1

U.S. Department of the Interior
Bureau of Reclamation
Technical Service Center
Denver, Colorado

April 2006

REPORT DOCUMENTATION PAGE	*Form Approved* *OMB No. 0704-0188*

1. REPORT DATE (DD-MM-YYYY) 24-04-2006	**2. REPORT TYPE** Interim Final	**3. DATES COVERED** *(From - To)* October 2003 - November 2005

4. TITLE AND SUBTITLE Plant-Scale Engineering Design of Membrane Processes from Bench-Scale Measurements, Version 1	**5a. CONTRACT NUMBER** 03-FC-81-0918
	5b. GRANT NUMBER
	5c. PROGRAM ELEMENT NUMBER
6. AUTHOR(S) John Pellegrino and Kohn Phu	**5d. PROJECT NUMBER**
	5e. TASK NUMBER
	5f. WORK UNIT NUMBER
7. PERFORMING ORGANIZATION NAME(S) AND ADDRESS(ES) Department of Civil, Environmental, and Architectural Engineering, 428 UCB University of Colorado – Boulder Boulder, CO 80309-0428	**8. PERFORMING ORGANIZATION REPORT NUMBER**
9. SPONSORING/MONITORING AGENCY NAME(S) AND ADDRESS(ES) Bureau of Reclamation, Denver Federal Center, P.O. Box 25007, Denver, CO 80225	**10. SPONSOR/MONITOR'S ACRONYM(S)**
	11. SPONSOR/MONITOR'S REPORT NUMBER(S) DWPR Report No. 115

12. DISTRIBUTION/AVAILABILITY STATEMENT

Available from National Technical Information Service, Operations Division,
5285 Port Royal Road, Springfield, VA 22161

13. SUPPLEMENTARY NOTES

Final Report can be downloaded from Reclamation website: www.usbr.gov/pmts/water/reports.html

14. ABSTRACT

The initial components of a self-contained software application have been created to provide material balances (that is, the permeate and retentate flowrates and compositions) and the pump energy for plant scale reverse osmosis (RO), nanofiltration (NF), ultrafiltration (UF), and microfiltration (MF) membrane unit operations. The application modeling allows some input parameters to come from the data normally reported from bench-scale measurements performed in standard stirred-cell, crossflow (aka swatch) apparatus, or small hollow-fiber modules. The software application was developed using the LabView® programming environment.

15. SUBJECT TERMS

membranes, water treatment processes, modeling

16. SECURITY CLASSIFICATION OF:			**17. LIMITATION OF ABSTRACT**	**18. NUMBER OF PAGES**	**19a. NAME OF RESPONSIBLE PERSON** Saied Delagah
a. REPORT U	**b. ABSTRACT** U	**a. THIS PAGE** U			**19b. TELEPHONE NUMBER** *(Include area code)* 303-445-2248

Standard Form 298 (Rev. 8/98)
Prescribed by ANSI Std. Z39.18

Desalination and Water Purification Research and Development Program Report No. 115

Plant-Scale Engineering Design of Membrane Processes from Bench-Scale Measurements, Version 1

Prepared for the Bureau of Reclamation Under Agreement No. 03-FC-81-0918

by

John Pellegrino and Kohn Phu
University of Colorado
Civil, Environmental, and Architectural Engineering Department

U.S. Department of the Interior
Bureau of Reclamation
Technical Service Center
Denver, Colorado

April 2006

MISSION STATEMENTS

Disclaimer

Acknowledgments

We wish to recognize the major contributions made to this project by Kate Worster and Laura Richards. Kate Worster undertook the original ill-fated, thrust of developing this application as an Excel® Workbook, and then provided the initial LabView® VIs that evolved into the final product. Laura Richards undertook the thankless task of transcribing and creating fitting correlations for the aqueous electrolyte properties that were used in the subroutines. In addition, the Technical Project Manager, Mr. Saied Delagah, has continuously provided both intellectual input and moral support that allowed us to bring the effort to its current conclusion. This research was sponsored by the Desalination and Water Purification Research and Development Program of the Bureau of Reclamation.

CONTENTS

Page

Figures

Page

Tables

Page

SYMBOLS, ACRONYMS, AND ABBREVIATIONS

d	diameter of pipe
D	diffusivity
f (as subscript)	feed water
g-mol	gram-mole
k	boundary layer coefficient
L	liter
L	length
M	molar concentration
MF	microfiltration
mol	mole
NDP	net driving pressure
NF	nanofiltration
P	pressure
p (as subscript)	permeate
R	the ideal gas constant
Re	Reynolds number
RO	reverse osmosis
Sc	Schmidt number
Sh	Sherwood number
T	temperature
UF	ultrafiltration
vi	any of various subroutines of the LabView® program
V	velocity
MPa	megapascals
r (as subscript)	retentate, concentrate, or reject
V	volumetric flowrate
C	concentration
K	kelvins
ΔP	applied transmembrane pressure
μ	fluid viscosity
Π	osmotic pressure
ρ	fluid density

EXECUTIVE SUMMARY

The initial components of a self-contained software application have been created to provide material balances (that is, the permeate and retentate flowrates and compositions) and the pump energy for plant scale reverse osmosis (RO), nanofiltration (NF), ultrafiltration (UF), and microfiltration (MF) membrane unit operations. The application modeling allows some input parameters to come from the data normally reported from bench-scale measurements performed in standard stirred-cell, crossflow (aka swatch) apparatus, or small hollow-fiber modules.

The software application was developed using the LabView® programming environment. Though normally a data acquisition and process control software, LabView® provides many library routines (called VIs) that perform sophisticated mathematical functions. In addition, LabView® provides a built-in, graphical user interface for both input and output; can be used on Unix, MacOS, and Windows operating systems; applications can be distributed as compiled, run-only programs that do not require ownership of the LabView® software; and the application routines can be directly used to create an unlimited number of process "flow diagrams".

The purpose of the modeling software is to provide researchers, designers, and project managers with a tool to quantitatively assess the significance of technical advances that are often first described by reports of bench-scale measurements. This modeling tool can: i) enhance the accuracy and capability of sensitivity analyses done to focus research efforts, ii) reduce the time (and cost) to implement new technology and applications of existing technology, and iii) facilitate optimizing cost and/or design for different operating conditions. The proposed software should, eventually, be integrated with the Reclamation-sponsored WTCost© software.

The modeling software has several separate components including fitting correlations for the density, viscosity, and osmotic pressure of aqueous electrolytes. Mixtures are currently represented as perfect solutions. We have not incorporated any phase equilibrium considerations in this initial application. The model is primarily able to reduce experimental data in terms of an "effective medium" that represents the complex (or simple) mixture that the researcher used. That is, there will be one or two "key" solutes whose transport properties through the membrane fit the reported data based on the conditions that the experimenter used—for instance, this is similar to representing a mixture of natural organic matter (NOM) as a single molecular mass component. Importantly, the test solution can also have an "effective" flux decline character that will be defined in terms of empirical parameters. The membrane's solvent flux permeability can be defined based on the experimental results. These calculated parameters and properties will then be integrated (using a general shell balance) through a user-specified membrane system with a desired capacity and configuration to calculate

the local concentrations and pressure required over the course of time. The ultimate output will be the permeate and retentate (reject) flowrates and compositions, and the increase in pumping pressure over time that is required to keep the specified production rate. Temperature changes are not be included in this Version 1.

BACKGROUND

If we accept the conclusions of the Desalination Roadmap (2003), the development of viable, cost-effective, and technically efficient water supplies will include membrane processes for the foreseeable future. Membrane-based separations are an embodiment of the ideal separation processes. Accepting that premise, then it is clear that anything that reduces development time and cost will hasten the installation of viable water reclamation process equipment and will decrease the cost of the water produced. Better process design will not only lower the development costs incurred, but will also lowering the cost of capital and increase system reliability. In addition, process design tools that provide the means to assess the value of technological innovations, will help focus limited resources into the areas that will provide the greatest benefit and/or leveraging.

At present, the development of plant scale membrane installations are often slowed by the “cherished belief” that every new combination of water composition (quality) and membrane material and/or module requires extensive testing and validation through pilot scale. The belief that every new water recovery application needs to follow the exact same piloting processes often limits the number of membrane materials and process operating conditions that will be evaluated.

Process-modeling tools help create the means for extending lower-cost bench-scale measurements into “virtual pilot-scale evaluations.” Many more bench scale measurements can be done in a shorter period of time, which is desireable following Allgeier and Summers (1995), and therefore fewer pilot-scale evaluations need be performed with the optimum materials and under suitable process conditions to validate the design premises. This software model can be made widely accessible to maximize its impact on the development of new membrane technology—the scale-up modeling approach does not need to change as new membrane technology is developed, as long as the new technology is embodied in the bench scale tests.

Review of Membrane Process Modeling

Academic and industrial researchers have produced many outstanding fundamental modeling efforts. More specifically, in recent years very detailed numerical studies have been executed to predict the membrane filtration behavior of more and more complicated systems, including such fundamental aspects as solute and membrane pore-size distributions, fluid flow hydrodynamics, module non-uniformities, and variable fluid properties (for example, viscosity gradients). In addition, membrane manufacturers have their own proprietary, black-box engineering models that are used to recommend their membrane systems to customers. These prior contributions and resources will inform the proposed project, but have been developed for different goals and thus manipulate physical models that are not completely appropriate for the current purpose.

The engineering design of a membrane process includes at least three (3) levels of transport phenomena:

1. The first level is the transport of solvent and other species through the membrane (Mulder, 1992). This is the most fundamental level of membrane science and technology and has been predominately studied by academia in the current era (the last 40–50 years) of synthetic membrane development. The variety of models include a spectrum of approaches that incorporate solution-diffusion (Adam et al, 1983; Theil, 1990; Kataoka et al, 1991), frictional flow (Sourirajan and Matsuura, 1986), and hindered partitioning/diffusion (Deen, 1989; Schaep et al, 1999) which will cover the range of reverse osmosis, nanofiltration, ultrafiltration, and microfiltration. In fact, the most complete, and fundamental, form was presented by Mason and Lonsdale (1990), with which they show how all other membrane transport models directly result by making appropriate assumptions and neglecting terms. Nonetheless, for the modeling of this proposed project, we choose to use the "black box", non-equilibrium transport model initially developed by Kedem and Katchalsky (1958) and Spiegler and Kedem (1966). This modeling approach has been widely accepted especially when the parameters are experimentally measured (or estimated with minimum assumptions.)
2. The next level of transport concern is in the mass transfer that occurs in the fluid phase that is next to the membrane. It is well recognized that concentration polarization, colloid (or particle) deposition, and adsorption phenomena influence flux decline (fouling) as well as the solute and solvent transport through the membrane—and vice-versa. Unlike membrane transport, the study, prediction, and measurement of mass transfer (and prevention of flux decline) in membrane filtration has been the major pre-occupation of membrane technologists and researchers from, not only, academia but also industry and government in the last 20 years. One of the earliest reviews of this subject was presented by Brian (1967) (for RO) and one of the most recent by Bowen (1995) is more broadly applicable. In general, a robust description of the concentration of solutes at the membrane interface is determined by solving a form of the advection-diffusion equation in the channel next to the membrane. Alternatively, a less detailed approach can be taken in which a "lumped" boundary-layer mass transfer coefficient is used to describe the change in solute concentration between the bulk fluid and the membrane interface, as done by Pradanos et al (1995).

In this case, a correlation is used to calculate the effective mass transfer coefficient. The description of the hydrodynamic environment is critical to this type of model and the effect of turbulence promoters must be adequately included, as shown by DaCosta (1993).

3. The final level of transport concern is the extension of the above mass transfer analysis to integration over the entire channel (or tube) length. When this is done, the prediction of the flowrates and compositions from complete elements, series of elements, and entire membrane process trains can be made. Many academic and industrial studies have been published on this topic. In the context of RO, the usefulness of short cut models (Sirkar et al, 1982, 1983; Evanelista 1985) have been recognized and successfully applied in proprietary software (Dow/FilmTec) and in academic studies to optimize process configuration (Evangelista, 1989). More complex models that include pressure drop in the module and variations in 10 geometry and mass transfer coefficient, and that require numerical solutions, have been developed and applied to RO (Wiley et al, 1985; El-Halwagi et al, 1996). Considering NF and UF, a variety of numerical modeling developments that include concentration polarization and particle deposition over an integrated channel geometry have been reported (Bhattachajee et al., 2001; Bacchin et al., 2002), with the recent NF-PROJECT (Noronha et al., 2002) being the most closely aligned with the objectives of this proposal.

Norona et al. (2002, 2003) have developed a computer simulation (NF-PROJECT) which uses as its input parameters the experimentally-obtained data from measurements on 2.5” × 40” elements. They fit the data from these measurements to the parameters for an irreversible thermodynamic model (Spiegler and Kedem, 1966) and, with several other phenomenological equations, perform an isothermal, steady state analysis of a process train of membrane elements. They have reported the use of this simulator to optimize the energy cost, permeate quality, and product flow The authors don’t describe their actual algorithm except that it is a numerical calculation (versus) analytical.

The current project builds very closely off the work of Norona et al. (2002, 2003), with the additions that: i) we wish to incorporate flux decline mechanisms due to adsorption and deposition, as well as, concentration polarization; ii) we will create an interface that can work with bench-scale (“swatch”) measurements collected in a variety of ways; iii) we will facilitate the adaptation of the software to all the pressure-driven membrane filtration processes; iv) we will build in a framework to extend the simulation to non-isothermal and unsteady-state operation (i.e., cleaning cycles); and, most importantly, v) the simulation tool will be directly available for Reclamation and their constituency to use.

CONCLUSIONS AND RECOMMENDATIONS

The development of this software application needs to be continued. There is still significant programming needed to complete even the simple RO design case without fouling. The major items include finishing the iterative approach of linking together elements (and the steps within elements), as well as the use of the mixed solutes properties. The next step after that would be to develop a way to link together multiple elements into a process train. The most straightforward approach is to define a fixed number of possible configurations and allow the user to choose among these.

In addition, we need to incorporate the fouling modeling, which is a very significant amount of further programming development because of the unsteady-state aspects.

The full program structure developed for the RO will be directly transferable to MF, UF, and NF. Only the transport equations and input parameters would need to be modified.

Comparison between the model application created in this project and the commercial offerings from membrane vendors should also be part of a future project.

RESULTS

Overview

As requested by Reclamation at the contract award, we had focused on developing an Excel® workbook environment that facilitates partitioning full membrane elements into smaller, discrete mass transfer units and solving the conservation equations over these spatial elements in a step-wise and iterative fashion for each time step.

Excel® Workbook Modeling Code Problem

Aside from a slightly different method of solving for the final variables for one element, the integration approach (summation of multiple divisions of one membrane element versus solving the entire membrane element as one mass transfer step) was not as successful when computing the equations with the macros. The main deterrents were the generation of several errors in Microsoft Excel®. These unsolved errors often caused the program to crash. After much deliberation and repeated attempts to correct these errors, it was concluded that there may be inherent limitations to using the Microsoft Excel® Solver Add-In as part of a set of nested calculations. The inter-relationships between the variables overwhelms Excel’s ability to compute the final iterations using macros and display them in a single output column.

Current Approach

We switched to a more suitable programming environment that is as user friendly as Microsoft Excel®, and also meets the program interface criteria. It is National Instrument’s LabView®. We followed the same algorithm structure that is described in Appendix 1.

Some of the advantages to using LabView® are that graphical user interface is more user friendly, the program is more capable of handling large loop and iterative calculations, and the results can be outputed in other programming languages or programs such as C+ and Microsoft Excel®. An application file with the model can be created and distributed quite easily (across multiple platforms), and does not require the expense of buying the full LabView® Development Environment. The application file will also be resistant to user tampering and unintentional changes. Reclamation will have the Full Development version of the model and can make any changes in future versions.

Several initial LabView® subroutines (called vi’s) have been created (these are described in Appendix 1), that calculate the previously outlined equations for an element with multiple sub-sections—which had caused many problems in the Excel® environment—and, as of this time, the current version has no errors. The immediate benefit to using the LabView® programming environment is the production of a program that not only works but is also stable and consistent, which Microsoft Excel® has not been. In addition, it will be easier to implement the use of collocation methods, to solve the entire mass and pressure balance in membrane elements on a global basis, in the LabView® environment. This collocation approach will take a future new project to develop and has some uncertainties, but will probably be a more robust software tool if successful.

The following list are the primary tasks and their current status:

- Task 1a. Develop the time-dependent, shell-balance, engineering design equations that include the pertinent macroscopic phenomena at a differential level. These include key solute component(s) permeability (1 component done); the solvent permeability (done); the hydrodynamic mass transfer coefficient (done); and the three main modes of flux decline (not started).
- Task 1b. Define the step size (for both membrane area and time integration) approaches for various types of membrane elements and module configurations, including consideration of overall plant size (done for spiral wound elements, not started for hollow fiber units).
- Task 1c. Develop the models for defining: i) the feed side mass transfer coefficient and ii) the pressure drop through an element/module (done).

- Task 1d. Define the integration algorithm for performing the summation of the material balance through each single element in a series and checking its convergence accuracy (simple forward difference method done).
- Task 1e. Develop a set of experimental data to input into the model for benchmark testing (done).
- Task 1f. Create a complete set of default parameters for all the model input variables (in progress).
- Task 1g. Create the Excel® workbook application using the specifications from subtasks 1a-f (effort using Excel® workbook has been cancelled in favor of using LabView® visual programming environment—this work is in progress).
- Task 1h. Beta test the Excel® workbook application with a selected data set that includes both bench-scale and pilot-scale measurements over extended periods of time (not begun).

Subprograms (vi's)

Labview® calls its subprograms vi's. Appendix 1 contains a detailed description of the vi's including the equations, definitions of the variables, and how the subprogram executes.

Benchmarking Data

We illustrate a reverse-engineering analysis of an arbitrarily chosen vendor's (Hydranautics SWC-2521 RO) specifications for a membrane element in Appendix 2. This was done in order to make comparisons with bench-scale data and the modeling algorithm results—and to facilitate extrapolation of that membrane to other process conditions.

Vendor Software

We need to compare and contrast our design modeling development with the vendor software tools available for RO systems. We have started with ROSA 5.3 (Dow- FilmTec). The initial results are shown in Appendix 3.

Physical Property Data

We are transcribing literature data of physical properties for representative species (salts, water, macromolecules, and solutions thereof) into electronic (spreadsheet) formats and fitting correlating equations to be used in process design models. These data include transport and volumetric properties of water as a function of temperature and pressure; density and activity coefficients for representative electrolytes and organic molecules in order to estimate osmotic pressures as a function of recovery. We have included the correlations in Appendix 4 and are included as subprogram vi's.

Modeling Approach

This section presents the overall algorithm and general modeling equations for performing stepwise material and energy (pressure) balances across a spiral-wound membrane element.

Membrane Element Geometric Model

We first consider unrolling a spiral-wound element as depicted in Figure 1. The overall flows are depicted and we consider discretizing the membrane into n sequential, differential area elements (a similar approach to Finite Element Methods) for further analysis as in Figure 2. Initially, we ignore any edge effects and the permeate side's composition effect on the mass transfer from the feed side of a semi-permeable membrane—though this assumption is easily relaxed. For the initial calculation scheme we make the pseudo-steady-state approximation for each time step.

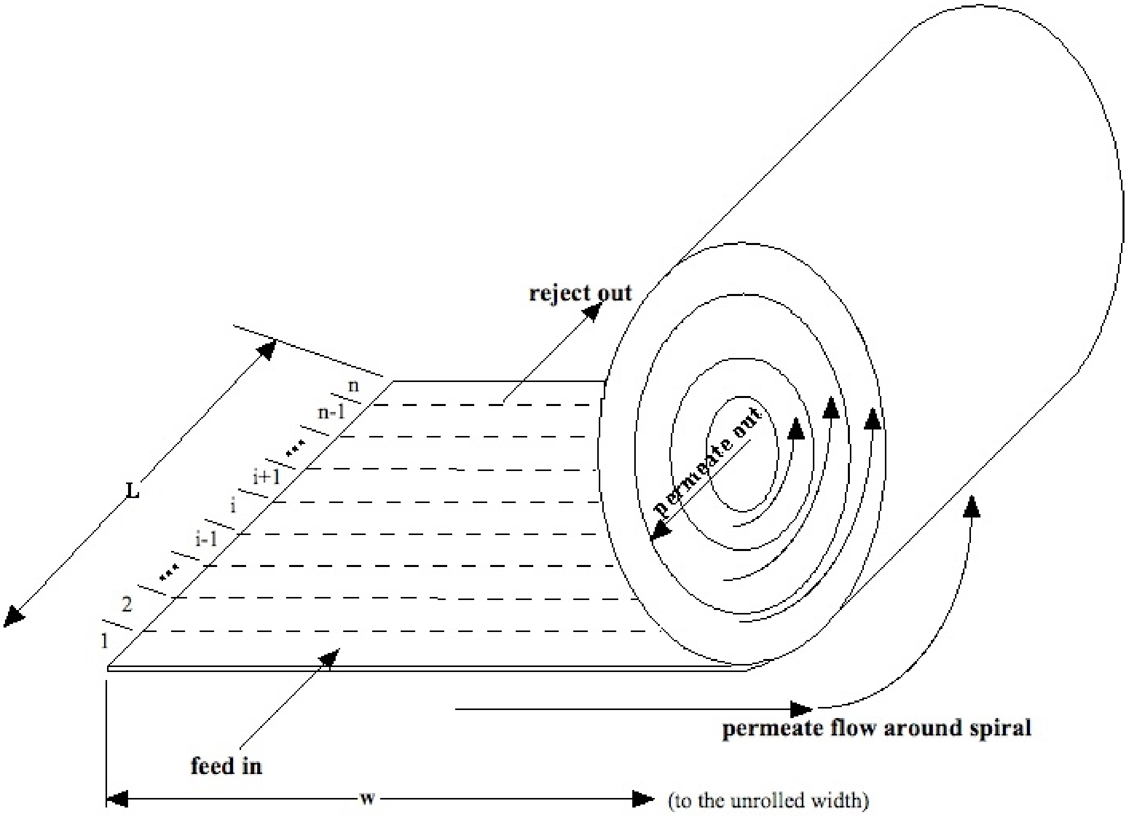

Figure 1. Unrolling a spiral-wound element.

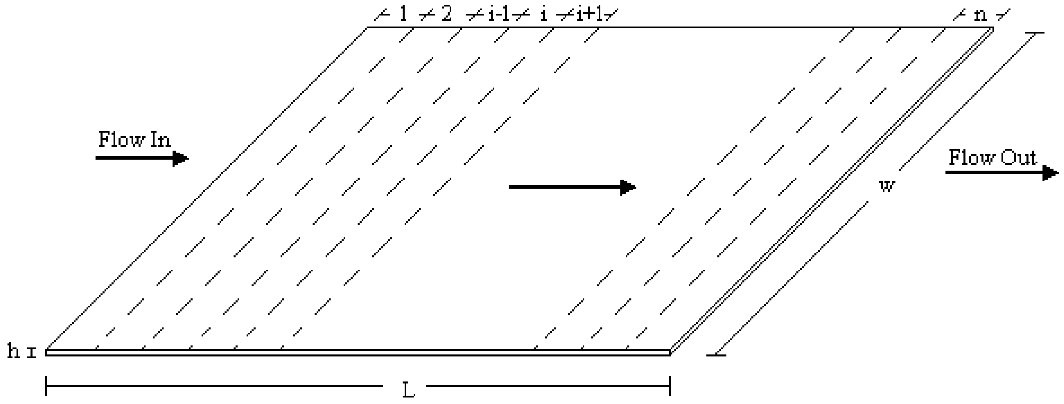

Figure 2. Division of membrane into sections (calculation-elements).

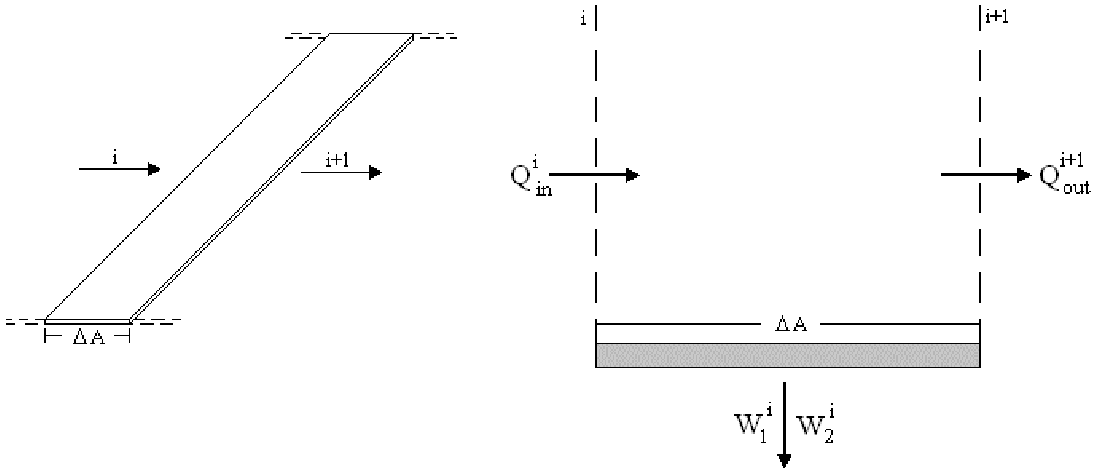

Figure 3. An individual area element; top view (left), side view (right).

Referring to Figure 3 we see that the differential membrane (or mass transfer) area is given by the following equation:

$$\Delta A = w\Delta L \tag{1}$$

where ΔL is determined by the degree that we discretize the overall element length, L. (N.B., We will need to evaluate the process design result's sensitivity to the choice of ΔL but, initially, we will use ~15 cm as a starting value. Thus, one would need to increase the size of the problem (that is, the number of calculation area elements) as the length of the full membrane element increases. For example, the number of differential area elements would be $n = L/15$, where L is given in centimeters.)

The mass balance is depicted in the RHS of Figure 3, where Q is the flow in the feed channel and W_1 and W_2 are the mass flows of water and solute (for example, NaCl) that permeate the membrane. The mass flows through the membrane are given (at any time t) by the specific flux equations and are coupled to the overall mass balance—in an iterative sense—by the compositions.

The Reynolds number (Re) will be calculated using Eq. 2. The cross-sectional area for flow is $A_x = h \cdot w$ (where h is the height of the feed channel —determined by the spacer thickness). The superficial velocity in each area element is given by $v = (Q^i + Q^{i+1})/(2A_x)$ and will be coupled with the fluid's density (ρ) and viscosity (μ).

$$\mathrm{Re} = \frac{v d_h \rho}{\mu} \tag{2}$$

The Re will be used with the appropriate correlations to determine the mass transfer coefficient and the frictional component of hydraulic pressure drop in the area element.

Net driving pressure

After calculating the mass transfer coefficient and frictional pressure loss, the Net Driving Pressure (NDP) must be applied to the differential area element to determine the permeate fluxes. The NDP is found by subtracting the pressure head of the permeate (P_p) and the osmotic pressure of the feed (Π_f) from the average of the incoming and outgoing feed pressure (P_f) and the osmotic pressure of the permeate (Π_p).

$$NDP = P_f + \Pi_p - P_b - \Pi_f \tag{3}$$

The Van't Hoff equation will be used for osmotic pressure of larger solutes present as dilute species.

$$\Pi = \frac{CRT}{M} \tag{4}$$

The osmotic pressure Π is in pascals and is calculated from the solute concentration (C) in moles per liter, temperature (T) in kelvins, the ideal gas constant (R), and the molecular mass of the solute (M) in grams per mole. For the electrolytes the correlations described in Appendix 4 are used.

Concentration

The concentrations of both the solvent and solute were required for all major calculations and are therefore important items to calculate correctly when converting units. The best estimates of real solution densities are being incorporated in order to make certain that mass and molar balances are done correctly. Even though fluxes are reported on a volumetric basis, the transport equations are really only accurate on a molar basis.

Mass transfer coefficient

The correlation approach described by DeCosta (1993) is incorporated employed to calculate the mass transfer coefficients in channels and the frictional pressure losses of the system. In conjunction with dimensional analysis, the Sherwood

(Sh), Schmidt (Sc), and Reynolds (Re) numbers were used to compute the mass transfer coefficient (km), which is the rate of mass transfer per unit area per unit concentration.

$$S_h = \frac{kd_h}{D} \tag{5}$$

$$S_c = \frac{\mu D}{\rho} \tag{6}$$

$$k_m = \frac{\dot{m}}{A_m(C_i - C_{i+1})} \tag{7}$$

The equation for the mass transfer coefficient consists of $\dot{m}$, which is the mass flow rate in units of kilograms per second; (C_i –C_{i+1}), which is the concentration of A_m in moles per cubic meter; and A_m, which is the area of the membrane section in square meters, thus giving the mass transfer coefficient units of meters per second.

Code Structure (current programming flowsheet)

A preliminary outline of the problem was used to create a base structure of the necessary program code. This base structure's framework was laid out in a flowchart format using Microsoft PowerPoint. In addition to following the number references from the text version of the code outline, all of the flow charts utilize the same color coding for their boxes defining the various different types and parts of the code (Figure 4).

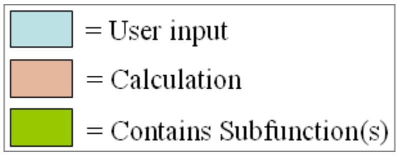

Figure 4. Flowchart color code.

The ideal case of steady state example was first modeled and broken down into sections that required sub-functions, user inputs, and program defined constants Figure 5.

Each of the boxes designated as containing subfunctions (green) are also outlined in the following flowcharts Figures 6 to 10.

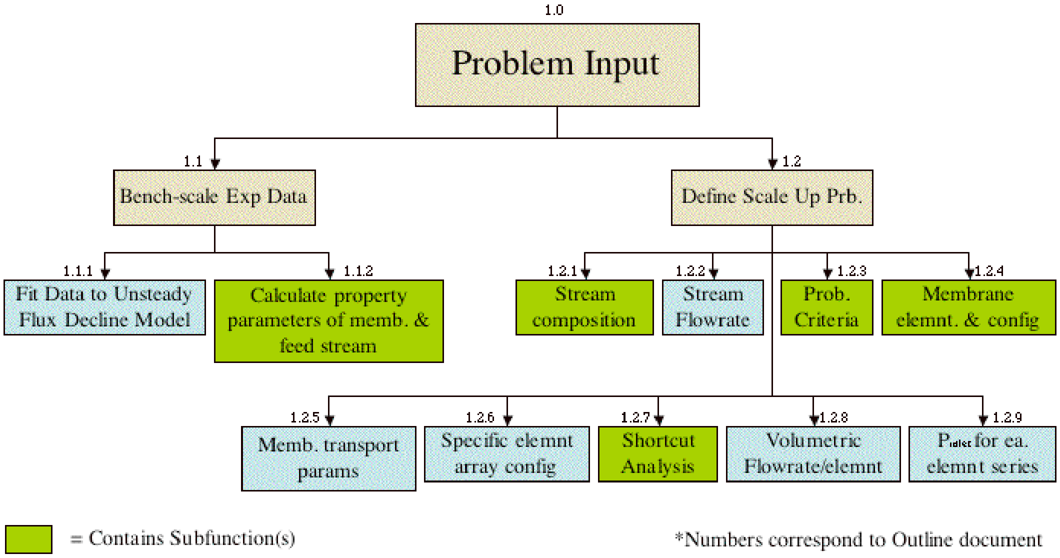

Figure 5. Code flowchart of steady state problem.

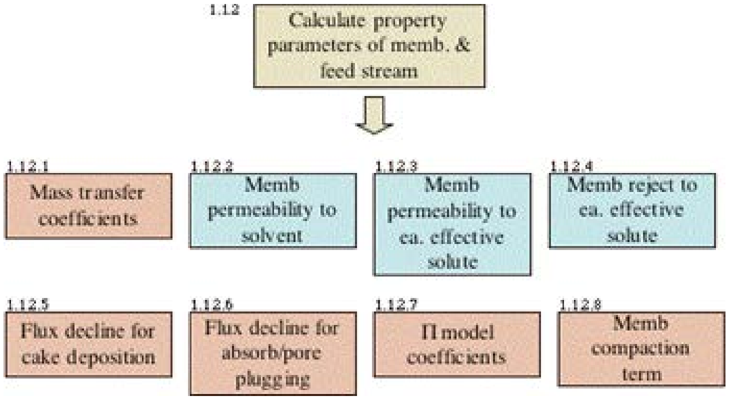

Figure 6. Outline of subfunction for calculation of intrinsic property parameters of the membrane and the feed stream.

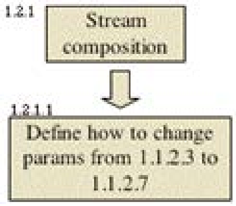

Figure 7. Outline of subfunction for stream composition.

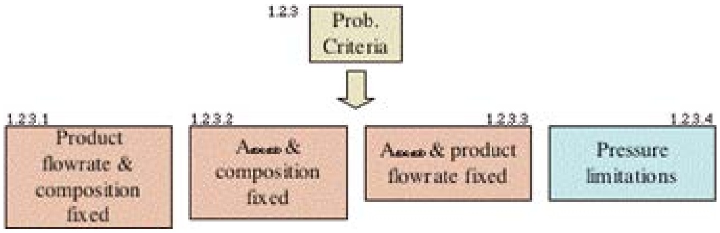

Figure 8. Outline of subfunction for specifying problem criteria.

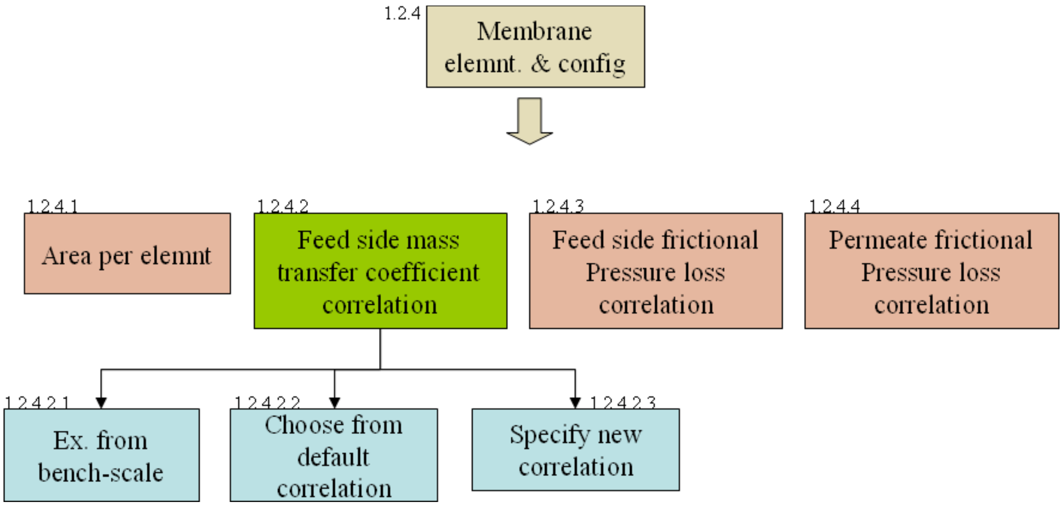

Figure 9. Flowchart for specifying the properties of the membrane elements.

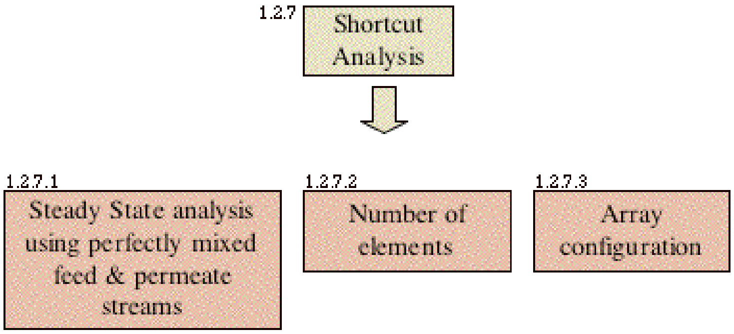

Figure 10. Flowchart for shortcut analysis to develop the initial starting guesses.

Once an ideal (perfectly mixed) steady state case and its respective subfunctions are modeled, a stepwise modeling (using the pseudo-steady-state approach) using the same methodology, numbering conventions, and color codes as described above for the steady state case is done. The time-dependent (pseudo-steady state approach) flowchart for an element are shown below as Figures 11 and 12.

For a time dependent problem, a pre-processor (in the problem input) will define the way to proceed in doing multiple time-steps. But, in general, each time-step will require solution of the pseudo-steady problem with changing initial conditions, until either a convergence criteria is reached, or a specified amount of time has passed.

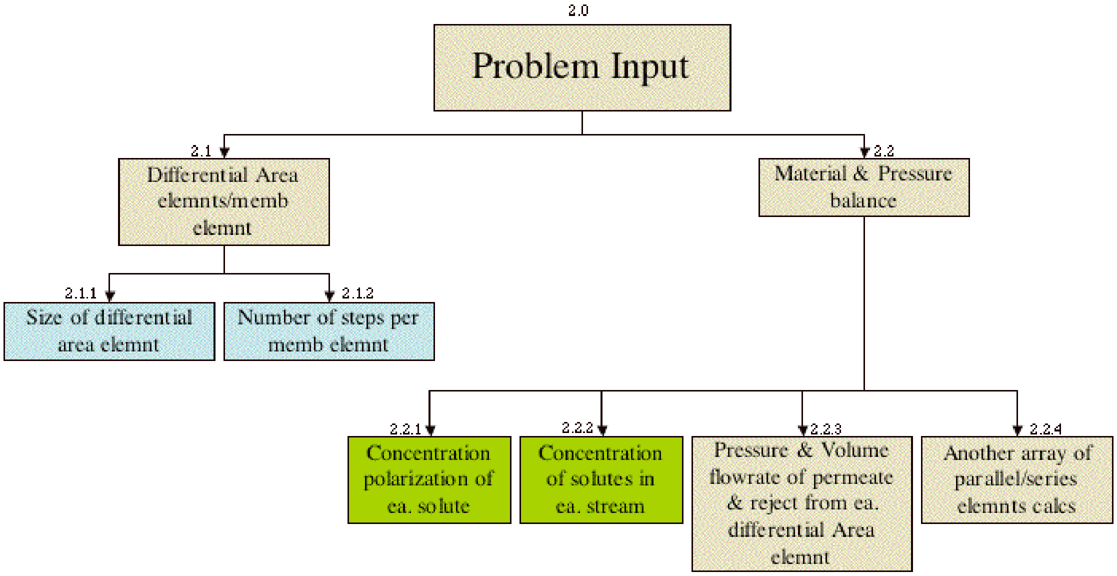

Figure 11. Flowchart for the pseudo-steady-state problem.

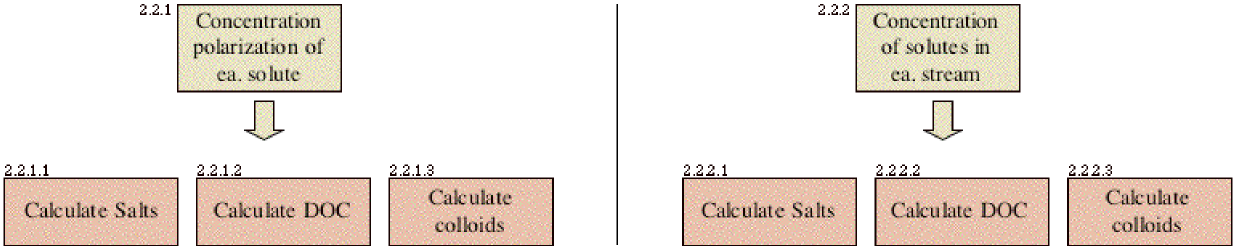

Figure 12. Flowchart for subfunctions to calculate the concentration polarization of each solute (left) and the solute material balance in each step (right).

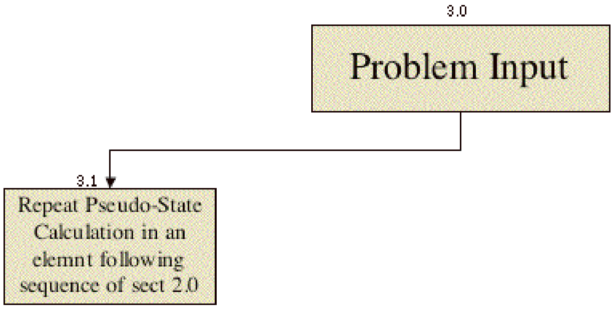

Figure 13. Outline of next step in the problem.

CURRENT OVERALL MODEL

The following “screenshot” presents the current topmost level. It is called the “Differential Unit.vi”. The values in the input boxes are the current defaults.

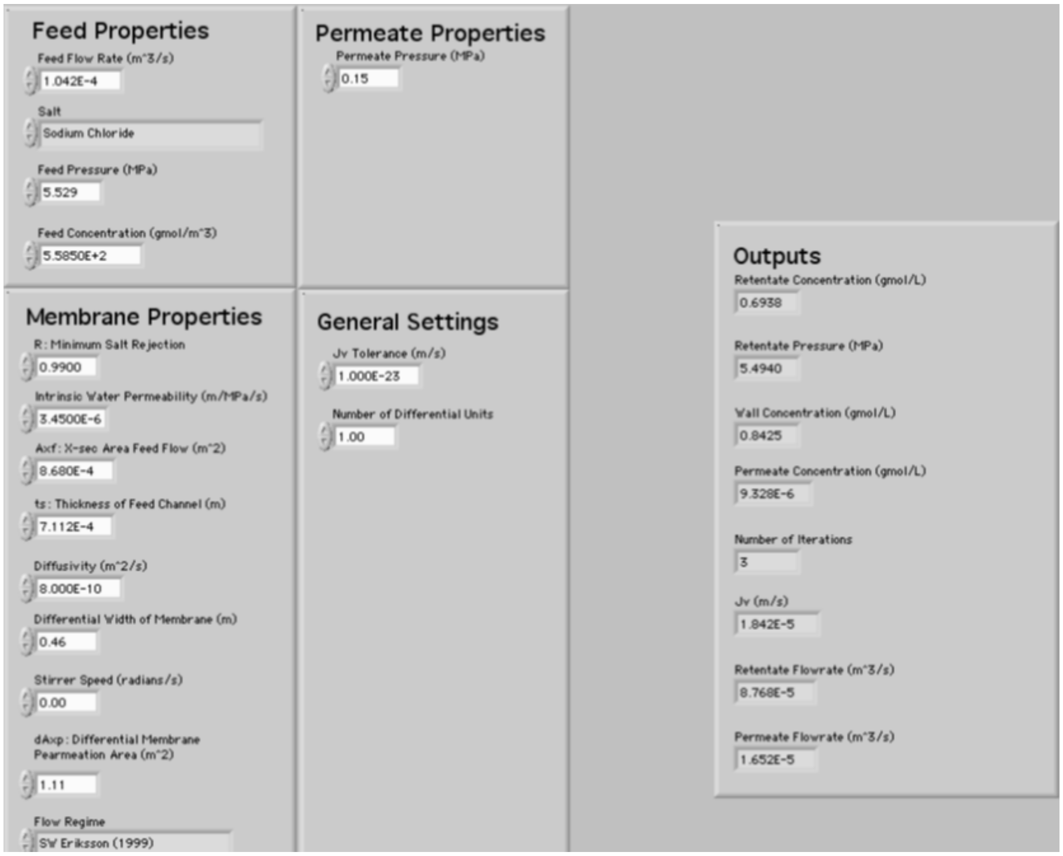

Feed Properties

Feed Flow Rate (m^3/s)
1.042E-4

Salt
Sodium Chloride

Feed Pressure (MPa)
5.529

Feed Concentration (gmol/m^3)
5.5850E+2

Permeate Properties

Permeate Pressure (MPa)
0.15

Membrane Properties

R: Minimum Salt Rejection
0.9900

Intrinsic Water Permeability (m/MPa/s)
3.4500E-6

Axf: X-sec Area Feed Flow (m^2)
8.680E-4

ts: Thickness of Feed Channel (m)
7.112E-4

Diffusivity (m^2/s)
8.000E-10

Differential Width of Membrane (m)
0.46

Stirrer Speed (radians/s)
0.00

dAxp: Differential Membrane Pearmeation Area (m^2)
1.11

Flow Regime
SW Eriksson (1999)

General Settings

Jv Tolerance (m/s)
1.000E-23

Number of Differential Units
1.00

Outputs

Retentate Concentration (gmol/L)
0.6938

Retentate Pressure (MPa)
5.4940

Wall Concentration (gmol/L)
0.8425

Permeate Concentration (gmol/L)
9.328E-6

Number of Iterations
3

Jv (m/s)
1.842E-5

Retentate Flowrate (m^3/s)
8.768E-5

Permeate Flowrate (m^3/s)
1.652E-5

This subprogram does the material and pressure balance on the inflows and outflows for an element. It needs significant further refinement, but right now does the calculations as described in Appendices 3 and 4 for a single element. The input is in the four leftmost sections and the output is in the rightmost section. To link together multiple elements the output from one element becomes the input to the next. A higher level subprogram (vi) is needed to do this and there are a variety of ways to approach this.

Feed Properties: The feed flow rate, composition, and pressure are the inputs.

Right now this subprogram (vi) works with a single “real” solute (and its properties) as the feed. This single “real” solute can be replaced by a “virtual” solute using the mixture properties as output from the Solution Properties.vi subprogram (see the following screenshot). This subprogram currently is set up for 3 components and uses a perfect mixture model (properties combine in proportion to their mole fractions). The properties (viscosity, density, osmotic pressure, and the conversion between mass fractions and molarity) are recalculated throughout the modeling in order to correctly account for the composition change. They are calculated at a constant temperature (20 °C), but that can (and will) be modified to use a general temperature dependency correlation based on perfect mixture theory.

Solution Properties.vi screenshot:

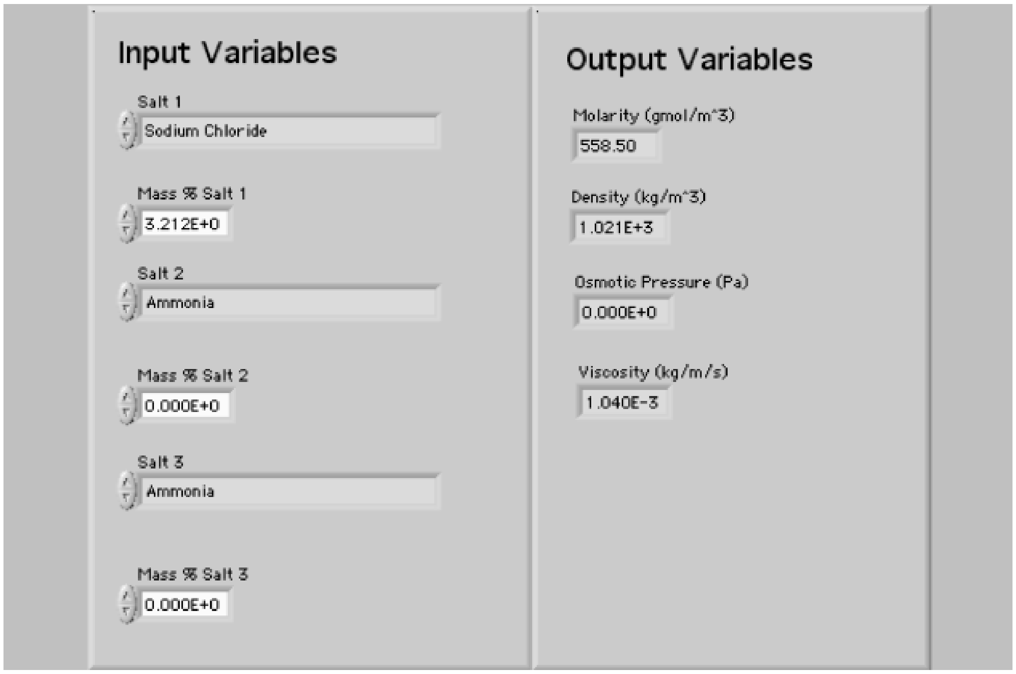

Input Variables

Salt 1: Sodium Chloride
Mass % Salt 1: 3.212E+0
Salt 2: Ammonia
Mass % Salt 2: 0.000E+0
Salt 3: Ammonia
Mass % Salt 3: 0.000E+0

Output Variables

Molarity (gmol/m^3): 558.50
Density (kg/m^3): 1.021E+3
Osmotic Pressure (Pa): 0.000E+0
Viscosity (kg/m/s): 1.040E-3

Permeate Properties: only the permeate pressure needs to be specified at this point because we are assuming that the permeate from each membrane element is collected separately (a good assumption with small spiral elements.)

Membrane Properties: these include the differential element's dimensions; the water permeability; the assumed salt (solute) rejection; the mass transfer model to use for calculating the boundary layer concentration; and the solute's bulk diffusion coefficient. Right now we assume a pressure drop along the element, in the future we will include a correlation to calculate it, and/or allow the user to input it as a variable.

General Settings: this is where items that relate to the calculation algorithm are input. The tolerance on iterating for the flux is the only operational value at present. The number of differential units is not used yet. It will be used to control the step size when working with longer elements.

APPENDICES

Appendix 1: Description of Some of the Working Subprogram vi's

Average.vi

Purpose: Computes average of up to five numbers.

Inputs: Number of Values, Value 1–5.

Outputs: Average.

Notes: vi assumes number of variables is correct.

Equations:

$$V_{avg} = \frac{\sum_i V_i}{i}$$

V_{avg} : Average value
V_i : i^{th} value
i : number of values

Boundary_layer_coeff2.vi

Purpose: Calculates the boundary layer coefficient in many different flow regimes/using different methods (SW Eriksson, Laminar Flow Between Parallel Plates, Laminar Flow in Round Tubes, Turbulent Flow in Stirred Batch Vessels, Turbulent Flow in Tubes 1 and 2).

Inputs: Diffusivity, viscosity, length, shear viscosity, diameter, avg. velocity, Reynold's number, stirrer speed, density, Schmidt number, height.

Outputs: Boundary layer coefficient.

Notes: Not all inputs have to be used for every model, vi does not check for this. User must make sure all required inputs have values.

Equations:

SW Eriksson

$$k = \frac{D \cdot \mathrm{Re}^{0.54} \cdot \mathrm{Sc}^{0.33}}{2 \cdot d}$$

k: boundary layer coefficient
D: diffusivity
Re: Reynolds number
Sc: Schmidt number
d: diameter of pipe

Laminar Flow Between Parallel Plates

$$k = 1.177 \cdot \sqrt[3]{\frac{U_c \cdot D^2}{h \cdot L}}$$

k: boundary layer coefficient
U_c: average velocity
h: distance between plates
L: length of plates

Laminar Flow in Round Tubes

$$k = 1.295 \cdot \sqrt[3]{\frac{2 \cdot U_c \cdot D^2}{d \cdot L}}$$

d: diameter of tube
L: length of tube

Turbulent Flow in Stirred Batch Vessels

$$k = 0.0443 \cdot \frac{D}{d} \cdot \left(\frac{\rho}{\mu \cdot D}\right)^{\frac{1}{3}} \cdot \left(\frac{\omega \cdot \mu \cdot d^2}{\rho}\right)^{\frac{3}{4}}$$

ρ: fluid density
μ: fluid viscosity

Turbulent Flow in Tubes 1

$$k = U_c \cdot \frac{0.0791}{2} \cdot Re^{\frac{-1}{4}} \cdot Sc^{\frac{-2}{3}}$$

Generally, to use this equation the Reynold’s number (Re) must be greater than 20,000.

Turbulent Flow in Tubes 2

$$k = 0.023 \cdot \frac{D}{d} \cdot Re^{0.83} \cdot Sc^{\frac{1}{3}}$$

Program Flowsheet:

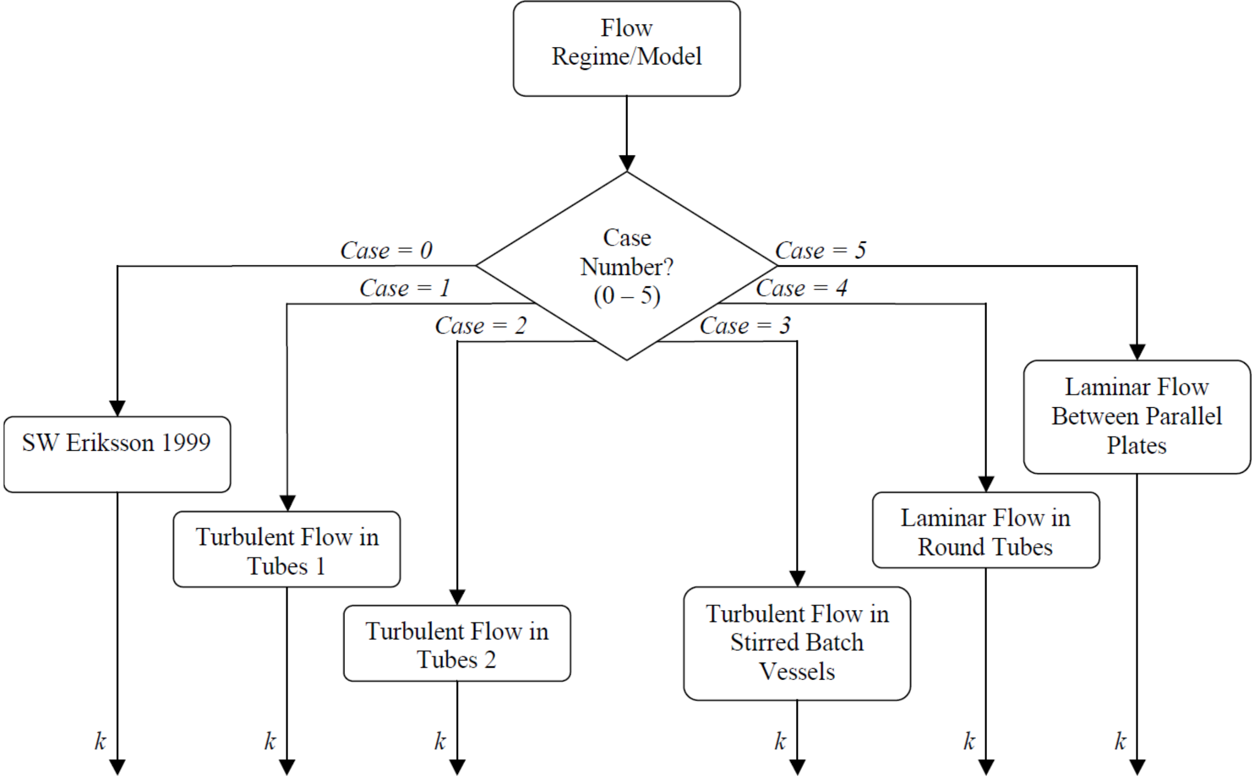

concentration_permeate.vi

Purpose: Calculates the concentration of the permeate using a very simplistic model.

Inputs: Retentate concentration, intrinsic rejection, solution flux, boundary layer coefficient.

Outputs: Permeate concentration.

Notes: N/A

Equations:

$$C_p = \frac{C_r \cdot (1 - R_o) \cdot e^{\frac{J_v}{k}}}{R_o + (1 - R_o) \cdot e^{\frac{J_v}{k}}}$$

C_p: permeate concentration
C_r: concentration retentate
R_o: membrane’s intrinsic rejection
J_v: flux through membrane
k: boundary layer coefficient

concentration_retentate.vi

Purpose: Calculates the concentration of the retentate using a very simplistic model.

Inputs: Boundary layer coefficient, intrinsic rejection, feed concentration, solution flux, recovery.

Outputs: Retentate concentration.

Notes: N/A

Equations:

$$C_r = \frac{C_f}{(1-\theta) + \frac{\theta \cdot (1-R_o) \cdot e^{\frac{J_v}{k}}}{R_o + (1-R_o) \cdot e^{\frac{J_v}{k}}}}$$

C_f: feed concentration
θ: recovery

concentration_wall.vi

Purpose: Calculates the concentration at the membrane wall.

Inputs: Boundary layer coefficient, intrinsic rejection, bulk concentration, solution flux.

Outputs: Membrane wall concentration.

Notes: N/A

Equations:

$$C_w = \frac{C_b \cdot e^{\frac{J_v}{k}}}{R_o + (1-R_o) \cdot e^{\frac{J_v}{k}}}$$

Cw: wall concentration
C : bulk concentration

differential_unit_guess.vi

Purpose: Calculates initial guesses for multiple conditions which are not given. This vi provides a starting point for differential_unit.vi. The values found by this vi are, for the most part, inaccurate as they are only guesses.

Inputs: Feed flowrate, salt, salt concentration, minimum salt rejection, intrinsic water permeability, feed pressure, permeate pressure, differential membrane permeation area, number of differential units.

Outputs: Retentate concentration, permeate concentration, retentate volumetric flowrate, retentate pressure, Jv, recovery.

Sub vi’s: Retentate_pressure.vi, Jv_Ro.vi.

Strategy: The vi first solves for the permeate concentration using the assumption that volume is additive (bad assumption unless fluid is incompressible). The vi then uses Retentate_pressure.vi which is a guess for the pressure drop along the membrane. After, the vi uses Jv_Ro.vi to solve for the flux. This flux will be off due to the fact that the initial guesses are off. The flux is then used to solve for permeate flowrate, which is in turn used to solve for retentate flowrate (doing a volumetric balance, assuming volume is additive once again). Retentate flowrate can then be used to solve for recovery. This then leads to retentate concentration being solvable.

Equations:

Volume Balance (assuming constant density)

$$C_p = C_f \cdot (1 - R_o)$$

C_p: permeate concentration
C_f: feed concentration
R_o: intrinsic rejection

Estimate for Permeate Flowrate

$$V_p = J_v \cdot dA_{xp}$$

V_p: permeate volumetric flowrate
J_v: flux through membrane
dA_{xp}: differential membrane cross sectional area

1st Estimate for Retentate Flowrate (assuming constant density)

$$V_r = V_f - V_p$$

V_f: feed volumetric flowrate

1st Estimate for Recovery

$$\theta = \frac{V_p}{V_f}$$

1st Estimate for Retentate Concentration

$$C_r = \frac{V_f \cdot C_f - V_p \cdot C_p}{V_r}$$

V_r: retentate volumetric flowrate

Program Flowsheet:

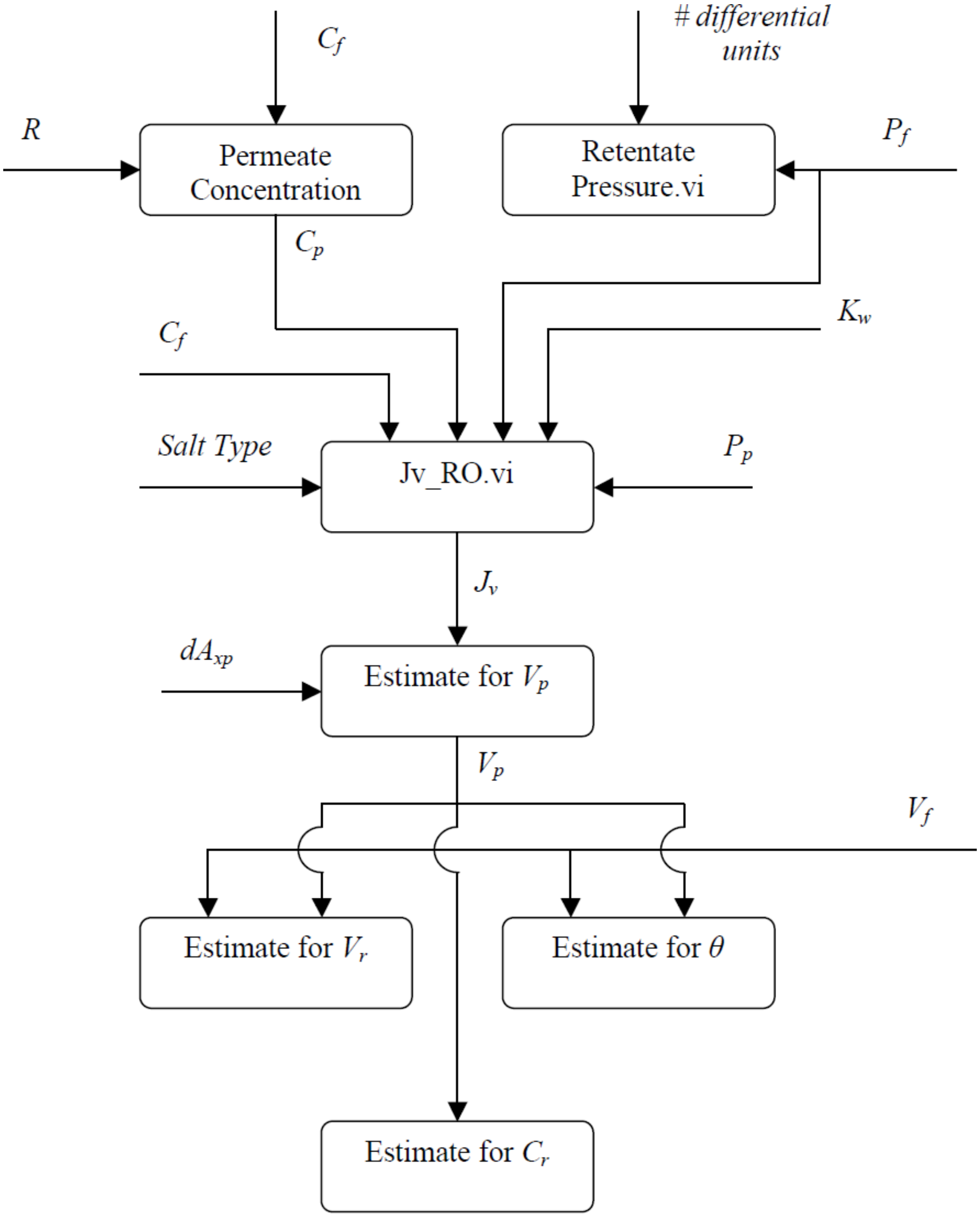

Differential Unit.vi

Purpose: Puts together all the basic vi's

Appendix 2: Benchmarking Analysis of Vendor Specifications (Hydranautics SWC-2521)

Pure water permeability is the first figure-of-merit determined when performing bench scale tests. This should be equivalent to the membrane's nominal intrinsic water permeability obtained when performing measurements containing solutes that are rejected by the membrane (at constant temperature). Temperature corrections would need to be made based on the change in viscosity and solute activity. Manufacturers typically publish data for an element test performed under specified conditions. In the following, we "deconstruct" a set of published data to show the algorithm that will be followed for translating (and verifying) bench scale data into parameters that will be forward-integrated in the modeling process.

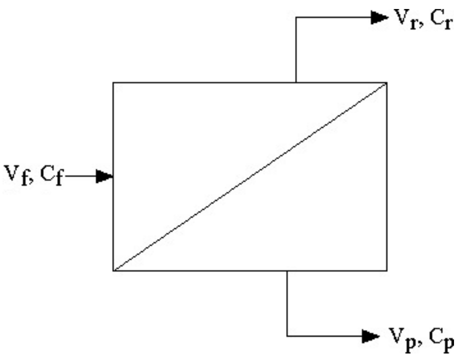

Figure A-1. Schematic of the generic membrane process.

We use Figure A-1 to define the design problem schematic. The variables (f = feed; r = retentate, concentrate, or reject; and p = permeate) are:

V_i = volumetric flowrate of stream i, (L/s)
C_i = concentration of stream i, (mol/L)
ρ_i = density of stream i, (kg/L)
ΔP = applied transmembrane pressure (psi)
ΔP_f = frictional pressure loss at flow conditions (psi)
J_v = water flux through the membrane (m/s)
$A_{x,P}$ = membrane area for permeation (m^2)

From the vendor specification sheet we use the following values for the parameters:

C_f = 32,000 ppm NaCl
ΔP = 800 psi (~5.5 MPa)
T = 25 °C
10% permeate recovery
$A_{x,P}$ = 12 square feet (~1.115 m^2)
V_p = 225 gallons per day (~0.9 m^3/d)

1) Calculate all flowrates:

$V_p = 1.0417 \times 10^{-5}$ m^3	$V_p = \frac{0.9\ \mathrm{m}^3}{\mathrm{d}} \cdot \frac{\mathrm{d}}{24\ \mathrm{h}} \cdot \frac{\mathrm{h}}{3600\ \mathrm{s}}$
$V_f = 1.0417 \times 10^{-4}$ m^3/s	Based on 10% recovery and assuming it was calculated on a volumetric basis and all flows were measured at atmospheric pressure and the same temperature (298 K). $V_f = \frac{V_p}{\mathrm{recovery}}$

$V_r = 0.9375 \times 10^{-4}\ \text{m}^3/\text{s}$	Using volumes to do the overall mass balance is the first assumption which can be corrected after calculating compositions. In the absence of certain knowledge of what the manufacturer used for their specifications, it's the best we can do to get started. $V_r = V_f - V_p$

2) Calculate all compositions:

As presented in the previous quarterly report, the physical properties of aqueous NaCl solutions were tabulated for our use. The densities in the following are based on that data. (See Table A-1, at end of this appendix).

$C_f = 0.5585$ mol/L	The 32,000 ppm is assumed to be based on mass, which is 0.032 g NaCl/g solution. The density of such a solution is ~ $\rho_f = 1.021$ kg/L. Thus: $C_f = \frac{0.032\ \text{kg NaCl}}{\text{kg solution}} \cdot \frac{1.021\ \text{kg solution}}{\text{L solution}} \cdot \frac{\text{mol NaCl}}{0.0585\ \text{kg NaCl}}$
$C_p = 5.585 \times 10^{-3}$ mol/L	Minimum salt rejection is specified as 99% and we assume that is the observed rejection. We use the molar concentration directly in the absence of better information. $C_p = C_f \cdot (1–0.99) = 0.5585 \cdot (0.01)M$
$C_r = 0.5812$ mol/L	The overall molar balance on the salt gives us C_r. $C_r = \frac{V_f \cdot C_f - V_p \cdot C_p}{V_r}$ $C_r = \frac{(1.0417\times10^{-4} \cdot 0.5585) - (1.0417\times10^{-5} \cdot 0.5585\times10^{-3})}{0.9373\times10^{-4}}$

3) Calculate average concentration in the bulk in the element:

$C_b = 0.5699$ mol/L	$\bar{C}_b = \frac{C_r + C_f}{2} = \frac{0.5812 + 0.5585}{2}$

4) Calculate the spacer dimension and open area for flow in the element:

We need to determine the average fluid velocity in the feed channel in order to determine the mass transfer coefficient to be used in calculating the wall concentration during the manufacturer's test. To do this, we need the actual cross-sectional area for flow.

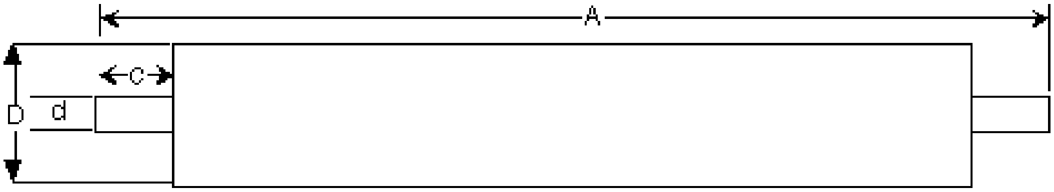

Figure A-2. Side view of spiral element.

The manufacturer's specifications are:

D = 0.061 m	A = 0.5334 m
d = 0.0191 m	c = 0.0305 m

We need to estimate the overall length of the spiral in order to determine the cross-sectional area for the feed flow to be passing through. Refer to the following Figure A-3 for our nomenclature and note that is somewhat different than that used in the report body when we are defining our flux modeling. This change in nomenclature is simply an immediate convenience.

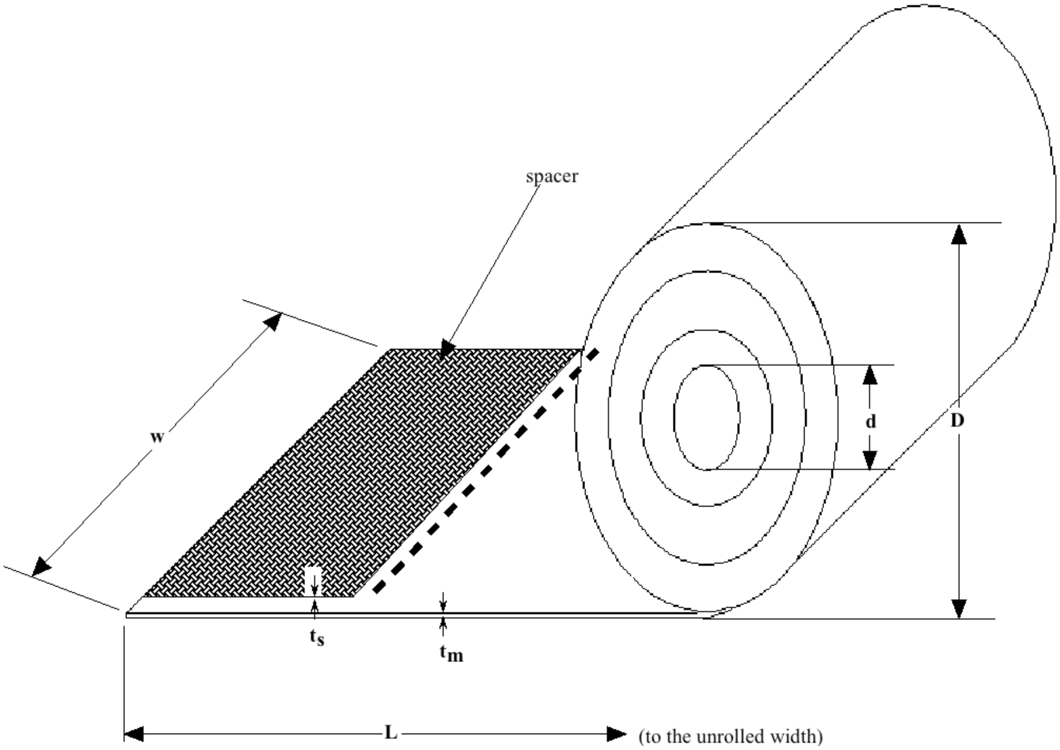

Figure A-3. Nomenclature applied to the SWC-2521 membrane.

We will use the following variable definitions:

L = the unwound length of a spiral envelope. A spiral envelope is two membranes enclosing a permeate carrier.

w = the width of membrane (spiral envelope).

t_m = the overall "compressed" thickness of the spiral envelope.

t_s = the thickness of the feed channel (presumed equal to the feed spacer thickness.)
D = the outer diameter of the spiral.
d = the core diameter for the permeate header.
c = the length of the core extensions.
n = the number of envelopes (and recognizing that each envelope has two membranes.)
$A_{x,T}$ = the total projected, cross-sectional area presented by the element to the feed.
$A_{x,M}$ = the total projected, cross-sectional area presented by the membrane envelope to the feed.
$A_{x,F}$ = the total projected, cross-sectional area available for feed flow (including the feed spacer).

We assume that the nominal 2.5” diameter element is made from one envelope.

$w = 0.4572$ m	We assume that some of the dimension A is used for the brine seals and glue lines (~0.6 inches or 0.01524 m). Thus $w = 0.5334 - 2\cdot 0.0305 - 0.01524$

The formula for the length of a spiral whose thickness is $t_m + t_s$ is given by:

$$L = \pi \cdot \frac{D-d}{2\cdot(t_m+t_s)} \cdot \frac{D+d}{2}$$

The membrane area for permeation must be equal to $L\cdot w$. Thus:

$$\frac{A_{x,P}}{2\cdot n} = w \cdot \frac{\pi}{2} \cdot \frac{D-d}{(n\cdot t_m + t_s)} \cdot \frac{D+d}{2}$$

where $2\cdot n$ is included because there are two membranes per envelope. We rearrange this to estimate $t_m + t_s$. And, we must assume something about the spacer. We assume a standard 28-mil (0.028”) diamond-shaped spacer (personal commun., Peter Eriksson, Osmonics-Desal, 1999). Thus, $t_s = 7.112\times10^{-4}$ m.

$t_m + t_s = 2.16\times10^{-3}$ m $t_s = 7.112\times10^{-4}$ m $t_m = 1.45\times10^{-3}$ m	$n\cdot t_m + t_s = w \cdot \frac{\pi}{2} \cdot \frac{2\cdot n}{A_{x,P}} \cdot \frac{D^2-d^2}{2}$ if we assume $n = 1$ $t_m + t_s = 0.457 \cdot \frac{\pi}{4} \cdot \frac{2}{1.115} \cdot 0.061^2 - 0.0191^2$
$A_{x,T} = 2.636\times10^{-3}$ m^2 $L = 1.2195$ m $A_{x,M} = 1.768\times10^{-3}$ m^2 $A_{x,F} = 0.868\times10^{-3}$ m^2	$A_{x,T} = \frac{\pi}{4}\cdot(D^2-d^2)$ $A_{x,M} = L\cdot t_m$ $A_{x,F} = A_{x,T} - A_{x,M}$

5) Calculate the superficial velocity through the feed channel and the bulk fluid mass transfer coefficient:

v = 0.114 m/s	v = the superficial velocity in the feed channel of the element $v = \frac{V_f + V_r}{2} \cdot \frac{1}{A_{x,F}} = \frac{1.0417 + 0.9375}{2 \cdot 8.68} \cdot \frac{10^{-4}}{10^{-4}}$
Re = 78.33	We are using the properties for a 0.613 M (35,000 ppm) solution; rigorous evaluation requires a trial-and-error approach $Re = \frac{v \cdot d_h \cdot \rho}{\mu}$ $d_h = t_s = 7.112\times10^{-4}$ m ρ = density of the bulk fluid, 1.025×10^{3} kg/m^3 μ = viscosity of the bulk fluid, 1.061×10^{-3} kg·m^{-1}·s^{-1}
Sc = 1,293.9	$\mathrm{Sc} = \frac{\mu}{\rho \cdot D}$ D = diffusion coefficient of salt in concentrated salt solution, 0.8×10^{-9} m^2/s
$k = 2.556\times10^{-3}$ m/s	we apply the mass transfer correlation presented by Eriksson (1999) $k = \frac{D}{d_h} \cdot a \cdot \mathrm{Re}^{b} \cdot \mathrm{Sc}^{0.33}$ a = 0.5 and b = 0.54

6) Calculate the average salt concentration at the membrane interface and the average osmotic pressure differences:

$\bar{C}_w$ = 0.5720 mol/L	Using the film theory approach: $\bar{C}_w = \bar{C}_b \cdot \frac{\exp(J_v/k)}{R_o + (1 - R_o) \cdot \exp(J_v/k)}$ $j_v = \frac{V_p}{A_{x,P}} = \frac{1.0417 \times 10^{-5}\ \mathrm{m}^3/\mathrm{s}}{1.115\ \mathrm{m}^2} = 9.34 \times 10^{-6}\ \mathrm{m}/s$ $\frac{J_v}{k} = \frac{9.34 \times 10^{-6}\ \mathrm{m/s}}{2.556 \times 10^{-6}\ \mathrm{m/s}} = 3.66 \times 10^{-3}$ R_o = 0.99
Π_w = 2.421 MPa Π_p = 0.022 MPa	The fit for the osmotic pressure (MPa) of NaCl solutions with concentration expressed as mol/L is: $\Pi = 3.8954 \cdot c + 0.5911 \cdot c^2$ $J_v = K_w(\Delta P - \Delta\Pi)$ $K_w = \frac{J_v}{(\Delta P - \Delta\Pi)} = \frac{9.34 \times 10^{-6}\ \mathrm{m}/s}{5.514 - (2.421 - 0.022)\ \mathrm{MPa}}$

5) Calculate the membrane's nominal intrinsic water permeability:

$K_w = 3\times10^{-6}$ m·MPa^{-1}·s^{-1}	The phenomenological flux equation is: $J_v = K_w(\Delta P - \Delta\Pi)$ the applied transmembrane pressure was set at 5.514 MPa $K_w = \frac{J_v}{(\Delta P - \Delta\Pi)} = \frac{9.34\times10^{-6}\ \mathrm{m}/s}{5.514-(2.421-0.022)\ \mathrm{MPa}}$

The following Table A-1 is extracted from the CRC Handbook of Chemistry and Physics, 71st Ed.

Table A-1. Bulk properties of aqueous NaCl solution at 293 K

Mass %, A (g/100 g)	**Relative density @ 293 K (kg/L)**	**Specific gravity (ρ_{H2O}= 0.99823)**	**Salt concentration (anhyd) (g/L)**	**Molarity, *M* (g-mol/L)**	**Water concentration (g/L)**	**Water displaced by salt (g/L)**	**Viscosity ($\times10^3$) (kg/m/s)**
0.1	0.9989	1.0007	1	0.017	997.9	0.3	1.005
0.5	1.0018	1.0036	5	0.086	996.8	1.5	1.012
1	1.0053	1.0071	10.1	0.172	995.3	3	1.021
1.5	1.0089	1.0107	15.1	0.259	993.8	4.5	1.029
2	1.0125	1.0143	20.2	0.346	992.2	6	1.037
3	1.0196	1.0214	30.6	0.523	989	9.2	1.053
3.5	1.0232	1.025	35.8	0.613	987.4	10.8	1.061
7.2	1.0500	1.0519	75.6	1.294	974.4	23.8	1.129
9.4	1.0662	1.0681	100.2	1.715	966	32.2	1.179
11.5	1.0819	1.0838	124.4	2.129	957	40.8	1.238
14	1.1008	1.1028	154.1	2.637	946.7	51.5	1.318
20	1.1478	1.1498	229.6	3.928	918.2	80	1.559
23	1.1721	1.1742	269	4.613	902	95.7	1.747
26	1.1972	1.1993	311.3	5.326	885.9	112.3	1.992

We have used this data to develop a density correlation which is needed to change mole or mass fractions to volumetric flow rates. The correlation is:

$\hat{\rho} = 55.426 - 0.44258x_2 - 95.156x_2^2$, where $\hat{\rho}$ is in gram-moles per liter and x_2 is the NaCl mole fraction.

HYDRANAUTICS
High Performance Membrane Products
A NITTO DENKO CORPORATION

Membrane Element SWC-2521

Performance:	Permeate Flow:	225 gpd (0.9 m^3/d)
	Salt Rejection:	
	Minimum	99.0 %

Type	Configuration:	Spiral Wound
	Membrane Polymer:	Composite Polyamide
	Nominal Membrane Area:	12 ft^2

Application Data	Maximum Applied Pressure:	1,000 psig (6.9 MPa)
	Maximum Chlorine Concentration:	< 0.1 PPM
	Maximum Operating Temperature:	113 °F (45 °C)
	Feedwater pH Range:	3.0 - 10.0
	Maximum Feedwater Turbidity:	1.0 NTU
	Maximum Feedwater SDI (15 mins):	5.0
	Maximum Feed Flow:	6 GPM (23 l/m)
	Minimum Ratio of Concentrate to Permeate Flow for any Element:	5:1
	Maximum Pressure Drop for Each Element:	10 psi

Test Conditions

The stated performance is initial (data taken after 30 minutes of operation), based on the following conditions:

32000 PPM NaCl solution
800 psi (5.5 MPa) Applied Pressure
77 °F (25 °C) Operating Temperature
10% Permeate Recovery
6.5 - 7.0 pH Range

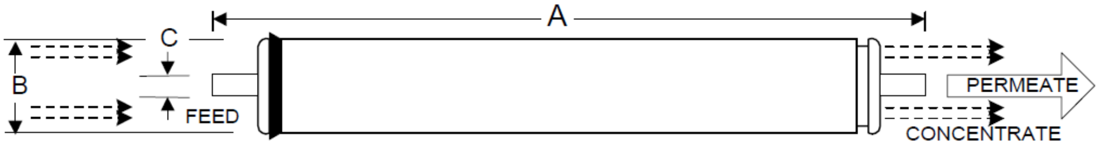

A, inches (mm)	B, inches (mm)	C, inches (mm)	Weight, lbs. (kg)
21.0 (533.4)	2.4 (61)	0.75 (19.1)	2 (0.9)

Core tube extension = 1.2" (30.5 mm)

Notice: Minimum permeate flow for individual elements 15 percent below listed flow. All membrane elements are supplied with a brine seal. Elements are vacuum sealed in a polyethylene bag containing less than 1.0% sodium meta-bisulfite solution, and then packaged in a cardboard box.

7/11/02

Appendix 3. Vendor Design Software: Program Comparisons

There are several reverse osmosis process simulators offered by equipment vendors. They include the Dow/Filmtec ROSA (a computer design program for designing plants with FILMTEC reverse osmosis membranes); GE Osmonics WINFLOWSTM (a computer design program for complex system configurations such as designs with feed bypass, recycle, two-pass, and two-stage configurations); and IMSDesign (a comprehensive membrane software design package that allows the user to design a membrane system using Hydranautics membranes).

ROSA 5.3

The ROSA version 5.3 commercial program was also run to compare with the results of the calculations from the Microsoft Excel® code. The following results were run for a reverse osmosis system under the same conditions as defined in the Microsoft Excel® code.

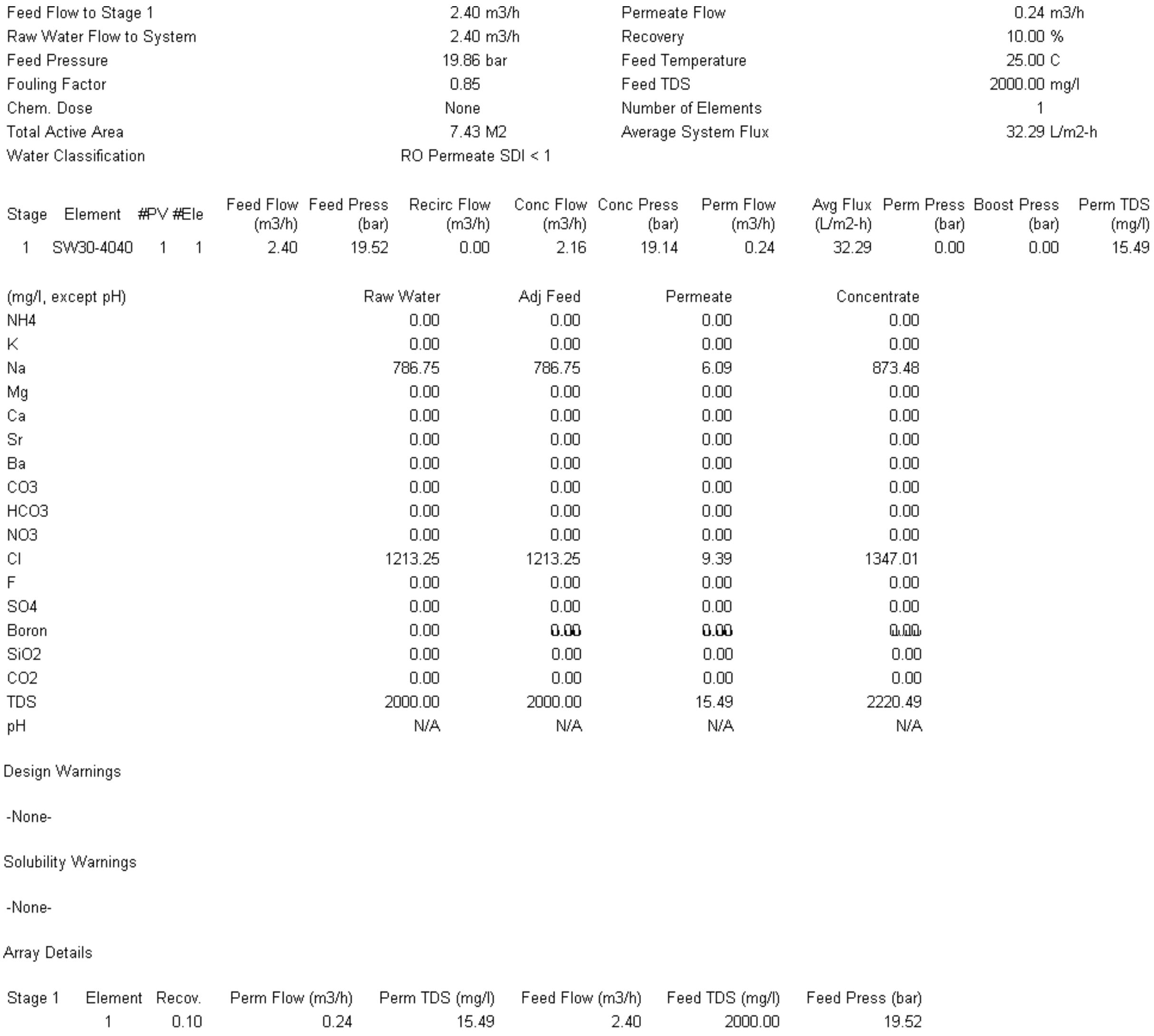

```
Feed Flow to Stage 1                        2.40 m3/h        Permeate Flow                     0.24 m3/h
Raw Water Flow to System                    2.40 m3/h        Recovery                          10.00 %
Feed Pressure                               19.86 bar        Feed Temperature                  25.00 C
Fouling Factor                              0.85             Feed TDS                          2000.00 mg/l
Chem. Dose                                  None             Number of Elements                1
Total Active Area                           7.43 M2          Average System Flux               32.29 L/m2-h
Water Classification                    RO Permeate SDI < 1

                          Feed Flow Feed Press Recirc Flow Conc Flow Conc Press Perm Flow  Avg Flux Perm Press Boost Press Perm TDS
Stage Element   #PV #Ele     (m3/h)      (bar)      (m3/h)    (m3/h)      (bar)    (m3/h)  (L/m2-h)      (bar)       (bar)    (mg/l)
  1   SW30-4040  1    1        2.40      19.52        0.00      2.16      19.14      0.24     32.29       0.00        0.00     15.49

(mg/l, except pH)              Raw Water     Adj Feed      Permeate      Concentrate
NH4                                 0.00         0.00          0.00             0.00
K                                   0.00         0.00          0.00             0.00
Na                                786.75       786.75          6.09           873.48
Mg                                  0.00         0.00          0.00             0.00
Ca                                  0.00         0.00          0.00             0.00
Sr                                  0.00         0.00          0.00             0.00
Ba                                  0.00         0.00          0.00             0.00
CO3                                 0.00         0.00          0.00             0.00
HCO3                                0.00         0.00          0.00             0.00
NO3                                 0.00         0.00          0.00             0.00
Cl                               1213.25      1213.25          9.39          1347.01
F                                   0.00         0.00          0.00             0.00
SO4                                 0.00         0.00          0.00             0.00
Boron                               0.00         0.00          0.00             0.00
SiO2                                0.00         0.00          0.00             0.00
CO2                                 0.00         0.00          0.00             0.00
TDS                              2000.00      2000.00         15.49          2220.49
pH                                   N/A          N/A           N/A              N/A

Design Warnings

-None-

Solubility Warnings

-None-

Array Details

Stage 1   Element  Recov.   Perm Flow (m3/h)   Perm TDS (mg/l)   Feed Flow (m3/h)   Feed TDS (mg/l)   Feed Press (bar)
             1      0.10               0.24             15.49               2.40           2000.00              19.52
```

As displayed above, the results are similar to the Microsoft Excel® results for a single element with zero sub-sections.

Appendix 4: Physical and Chemical Property Data Accumulation and Correlation

Physical properties of single component electrolyte solutions are being transcribed into digital format (spreadsheets) for several solutes. These databases will allow us to create correlation equations for density, viscosity, and osmotic pressure for the solutions formed during the membrane filtration process, including the concentration polarization effects. Thermodynamically consistent mixing rules will be applied to use this data for mixtures of electrolytes and/or electrolytes and organic species. Data for the following solutes have been added to our digital database. Thus far, we have used two main sources for the data, the CRC Handbook (1982) and Hamer and Wu (1972). The osmotic pressure data is currently being collected and verified for consistency.

Table A-2. Aqueous solutions properties at 293.15 K transcribed thus far

Solute	Concentration (anhyd g/L)	Density	Viscosity	Conductance
$BaCl_2$	5 – 332	Yes	Yes	Yes
$CaCl_2$	5 – 558.3	Yes	Yes	Yes
$CdCl_2$	10 – 1015.4	Yes	Yes	Yes
K_2CO_3	5 – 770.2	Yes	Yes	Yes
K_2SO_4	5 – 108.1	Yes	Yes	Yes
KCl	5 – 278.9	Yes	Yes	Yes
$KHCO_3$	5 – 280.4	Yes	Yes	Yes
LiCl	5 – 353.7	Yes	Yes	Yes
$MgCl_2$	5 – 382.9	Yes	Yes	Yes
$MgSO_4$	5 – 337.0	Yes	Yes	Yes
Na_2CO_3	5 – 173.6	Yes	Yes	Yes
NaCl	1 – 311.3	Yes	Yes	Yes
Seawater	5 – 166.8	Yes	Yes	Yes
$ZnSO_4$	5 – 188.9	Yes	Yes	Yes

Table A-3. Molarity (g-mol/L) as a function of mass percent salt
[Molarity = A×(Mass%)^2 + B×(Mass%)]

Salt	A	B
Ammonia	–0.0019	0.5814
Ammonium chloride	0.0005	0.187
Barium chloride	0.0006	0.0468
Cadmium chloride	0.0009	0.0465
Calcium chloride	0.0009	0.0876
Ethanol	–0.0005	0.2231
Lead nitrate	0.0004	0.0288
Lithium chloride	0.0015	0.2342
Magnesium chloride	0.001	0.1033
Magnesium sulfate	0.001	0.0817
Potassium bicarbonate	0.0007	0.099
Potassium carbonate	0.0008	0.0695
Potassium chloride	0.0009	0.1333
Potassium hydroxide	0.0019	0.1733
Potassium nitrate	0.0007	0.0981
Potassium sulfate	0.0005	0.0572
Sea water	- - - -	- - - -
Sodium carbonate	0.001	0.094
Sodium chloride	0.0013	0.1697
Sodium hydroxide	0.0027	0.251
Zinc sulfate	0.007	0.0613

This correlation simplifies performing process design material balances based on concentration units. Since molarity requires the solution density, this correlation implicitly includes the density variations for the different salt solutions, as well as their different molecular masses.

Table A-4. Relative density (kg/L) at 293 K as a function of mass percent salt
[Density = A×(Mass%)^2 + B×(Mass%) + C]

Salt	A	B	C
Ammonia	3.00×10^{-5}	–0.0043	0.99823
Ammonium chloride	-1.00×10^{-5}	0.0032	0.99823
Barium chloride	9.00×10^{-5}	0.0085	0.99823
Cadmium chloride	0.0001	0.0074	0.99823
Calcium chloride	5.00×10^{-5}	0.008	0.99823
Ethanol	-8.00×10^{-6}	–0.0013	0.99823
Lead nitrate	0.0001	0.0082	0.99823
Lithium chloride	1.00×10^{-5}	0.0056	0.99823

Salt	A	B	C
Magnesium chloride	4.00×10^{-5}	0.008	0.99823
Magnesium sulfate	6.00×10^{-5}	0.0099	0.99823
Potassium bicarbonate	3.00×10^{-5}	0.0064	0.99823
Potassium carbonate	4.00×10^{-5}	0.0088	0.99823
Potassium chloride	2.00×10^{-5}	0.0063	0.99823
Potassium hydroxide	3.00×10^{-5}	0.0086	0.99823
Potassium nitrate	3.00×10^{-5}	0.0062	0.99823
Potassium sulfate	3.00×10^{-5}	0.008	0.99823
Sea water	8.00×10^{-6}	0.0075	0.99823
Sodium carbonate	2.00×10^{-5}	0.0103	0.99823
Sodium chloride	3.00×10^{-5}	0.007	0.99823
Sodium hydroxide	-9.00×10^{-6}	0.0112	0.99823
Zinc sulfate	8.00×10^{-5}	0.0101	0.99823

Table A-5. Viscosity (Pa·s or $kg\cdot s\cdot m^{-1}$) as a function of mass percent salt

[Viscosity = A×(Mass%)^4 + B×(Mass%)^3 + C×(Mass%)^2 + D×(Mass%) + E]

Salt	A	B	C	D	E
Ammonia	- - - -	-1.00×10^{-8}	2.00×10^{-7}	1.00×10^{-5}	0.001002
Ammonium chloride	- - - -	2.00×10^{-9}	1.00×10^{-7}	-5.00×10^{-6}	0.001002
Barium chloride	- - - -	1.00×10^{-8}	-5.00×10^{-8}	1.00×10^{-5}	0.001002
Cadmium chloride	8.00×10^{-9}	-6.00×10^{-7}	1.00×10^{-5}	-8.00×10^{-5}	0.001002
Calcium chloride	9.00×10^{-9}	-4.00×10^{-7}	7.00×10^{-6}	-6.00×10^{-6}	0.001002
Ethanol	2.00×10^{-10}	-3.00×10^{-8}	8.00×10^{-7}	5.00×10^{-5}	0.001002
Lead nitrate	- - - -	- - - -	3.00×10^{-7}	3.00×10^{-6}	0.001002
Lithium chloride	3.00×10^{-9}	-9.00×10^{-8}	2.00×10^{-6}	3.00×10^{-5}	0.001002
Magnesium chloride	1.00×10^{-8}	-4.00×10^{-7}	6.00×10^{-6}	2.00×10^{-5}	0.001002
Magnesium sulfate	2.00×10^{-8}	-3.00×10^{-7}	4.00×10^{-6}	5.00×10^{-5}	0.001002
Potassium bicarbonate	- - - -	- - - -	4.00×10^{-7}	1.00×10^{-5}	0.001002
Potassium carbonate	4.00×10^{-9}	-2.00×10^{-7}	5.00×10^{-6}	-4.00×10^{-6}	0.001002
Potassium chloride	-3.00×10^{-10}	2.00×10^{-8}	-2.00×10^{-7}	-6.00×10^{-7}	0.001002
Potassium hydroxide	3.00×10^{-9}	-1.00×10^{-7}	3.00×10^{-6}	1.00×10^{-6}	0.001002
Potassium nitrate	- - - -	- - - -	2.00×10^{-7}	-6.00×10^{-6}	0.001002
Potassium sulfate	- - - -	- - - -	4.00×10^{-7}	1.00×10^{-5}	0.001002
Sea water	1.00×10^{-7}	-1.00×10^{-6}	5.00×10^{-6}	1.00×10^{-5}	0.001002
Sodium carbonate	- - - -	- - - -	5.00×10^{-6}	3.00×10^{-5}	0.001002
Sodium chloride	- - - -	4.00×10^{-6}	1.20×10^{-3}	1.71×10^{-1}	0.001002
Sodium hydroxide	1.00×10^{-8}	-5.00×10^{-8}	2.00×10^{-6}	6.00×10^{-5}	0.001002
Zinc sulfate	2.00×10^{-8}	-5.00×10^{-7}	5.00×10^{-6}	3.00×10^{-5}	0.001002

Table A-6. Conductance (mS/cm) as a function of mass percent salt

[Conductance = A×(Mass%)^5 + B×(Mass%)^4 + C×(Mass%)^3 + D×(Mass%)^2 + E×(Mass%)]

Salt	A	B	C	D	E
Ammonia	5.00×10^{-6}	-4.00×10^{-4}	9.50×10^{-3}	-1.19×10^{-1}	0.6406
Ammonium chloride	- - -	- - -	- - -	-1.43×10^{-1}	19.691
Barium chloride	- - -	- - -	- - -	-8.13×10^{-2}	8.4849
Cadmium chloride	1.00×10^{-6}	-2.00×10^{-4}	9.20×10^{-3}	-2.83×10^{-1}	4.3384
Calcium chloride	- - -	9.00×10^{-6}	-1.00×10^{-3}	-2.76×10^{-1}	14.636
Lead nitrate	- - -	- - -	1.20×10^{-3}	-1.02×10^{-1}	4.3442
Lithium chloride	- - -	- - -	3.80×10^{-3}	-5.43×10^{-1}	17.794
Magnesium chloride	- - -	- - -	4.20×10^{-3}	-5.49×10^{-1}	15.978
Magnesium sulfate	- - -	- - -	9.00×10^{-4}	-2.07×10^{-1}	6.4111
Potassium bicarbonate	- - -	- - -	- - -	-8.68×10^{-2}	8.1201
Potassium carbonate	- - -	- - -	- - -	-1.48×10^{-1}	12.358
Potassium chloride	- - -	- - -	- - -	-5.89×10^{-2}	14.839
Potassium hydroxide	- - -	- - -	- - -	-9.37×10^{-1}	39.832
Potassium nitrate	- - -	- - -	- - -	-9.79×10^{-2}	9.7801
Potassium sulfate	- - -	- - -	- - -	-1.68×10^{-1}	10.491
Sea water	- - -	- - -	- - -	-4.88×10^{-1}	15.12
Sodium carbonate	- - -	- - -	- - -	-3.54×10^{-1}	11.097
Sodium chloride	- - -	- - -	- - -	-2.50×10^{-1}	15.165
Sodium hydroxide	- - -	- - -	- - -	-1.76	49.943
Zinc sulfate	- - -	- - -	- - -	-1.18×10^{-1}	4.6183

REFERENCES

Adam, W.J., Luke, B., and Meares, P., The separation of mixtures of organic liquids by hyperfiltration, J. Memb. Sci., 13, 127-149 (1983).

Allgeier, S.C. and Summers, R.S., Development of a rapid bench-scale membrane test for the evaluation of nanofiltration performance. Proc. 1995 AWWA Membrane Technology Conf., Reno, NV (1995).

Bacchin, P., Si-Hassen, D., Starov, V., Clifton, M.J., and Aimar, P., A unifying model for concentration polarization, gel-layer formation, and particle deposition in cross-flow membrane filtration of colloidal suspensions, Chem. Eng. Sci., 57, 77-91 (2002).

Baruah, G. L., Venkiteshwaran, A., and Belfort, G., Global model for optimizing crossflow microfiltration and ultrafiltration processes: A new predictive and design tool, Biotechnol. Prog. 21 (4): 1013-1025 (2005).

Belfort, G., Membrane modules: comparison of different configurations using fluid mechanics, J. Memb. Sci. 35 (1988) 245-270.

Bhattachajee, S., Chen, J.C., and Elimelech, M., Coupled model of concentration polarization and pore transport in crossflow nanofiltration, AIChE J., 47, 2733-2745 (2001).

Bhattacharjee, C. and S. Datta, Numerical simulation of continuous stirred ultrafiltration process: An approach based on moving boundary layer concept, Sep. Sci. Technol. 38 (2003) 1749-1772.

Bowen, W.R. and Jenner, F., Theoretical descriptions of membrane filtration of colloids and fine particles: an assessment and review, Adv. Coll. Interface Sci., 56, 141-200 (1995).

Brian, P.L.T., Mass transport in reverse osmosis, Chap 5 in Desalination by Reverse Osmosis, U. Merten (ed.), The MIT Press, Cambridge, MA (1967).

CRC Handbook of Chemistry and Physics 62nd Edition, R.C. Weast ed., Concentrative Properties of Aqueous Solutions: Conversion Tables, CRC Press, Boca Raton, Fl, 1982.

DaCosta, A.R., Fluid flow and mass transfer in spacer-filled channels for ultrafiltration, PhD Thesis, University of New South Wales, Australia (1993).

Desalination and Water Purification Technology Roadmap: A Report of the Executive Committee, DWPR Report No. 95, USBR and Sandia Laboratories, (2003).

Deen, W.M., Hindered transport of large molecules in liquid filled pores, AIChE J., 33, 1409-1425 (1989).

Dow-FilmTec ROSA 5.3, http://www.dow.com/liquidseps/design/rosa.htm

El-Halwagi, A.M., Manousiouthakis, V., and El-Halwagi, M.M., Analysis and simulation of hollow fiber reverse-osmosis modules, Separation Science and Technology, 31, 2505-2529 (1996).

Elimelich, M. and S. Bhattacharjee, A novel approach for modeling concentration polarization in crossflow membrane filtration based on the equivalence of osmotic pressure model and filtration theory, J. Memb. Sci. 145 (1998) 223-241.

Eriksson, P., New design feed channel spacer in spiral-wound elements for pretreatment cost reduction, USBR Final Report Agreement No. 1425-97-FC-81-30006F (1998).

Evangelista, F., A short cut method for the design of reverse osmosis desalination plants, Ind. Eng. Chem. Proc. Des. Dev., 24, 211-223 (1985).

Evangelista, F., Design and performance of two-stage reverse osmosis plants, Chem. Eng. Processing, 25, 119-125 (1989).

Hamer, W. J. and Y. C. Wu, Osmotic coefficients and mean activity coefficients of uniunivalent electrolytes in water at 25 °C, J. Phys. Chem. Ref. Data, 1 (4) 1972.

Hwang, S-T. and K. Kammermeyer, Engineering aspects of membrane separations, Chap. 13 and Appendix C in Membranes in Separations, Robert E. Krieger Publishing Co., Inc., Malabar, FL (1984).

Kahdim, A.S., S. Ismail, and A. Jassim, Modeling of reverse osmosis systems, Desalination, 158 (2003), 323-329.

Kataoka, T., Tsuru, T., Nakao, S., and Kimura, S., Permeation equations developed for prediction of membrane performance in pervaporation, vapor permeation, and reverse osmosis based on the solution-diffusion model, J. Chem. Eng. Jap., 24, 326-333 (1991).

Kedem, O. and Katchalsky, A., Thermodynamic analysis of the permeability of biological membranes to non-electrolytes, J. Biochim. Biophys., 27, 229-246 (1958).

Masken, Fazilet, Optimization of reverse osmosis membrane networks, PhD Thesis (2000) University of New South Wales, Sydney, Australia (and references therein).

Mason, E.A. and Lonsdale, H.K., Statistical-mechanical theory of membrane transport, J. Memb, Sci., 51, 1-81, (1990).

Mulder, M., Basic Principles of Membrane Technology, Kluwer Academic Publishers, Dordrecht, NL, (1992).

Noronha, M., Mavrov, V., and Chmiel, H., Computer-aided simulation and design of nanofiltration processes, in Advanced Membrane Technology, N.N. Li, E. Drioli, W.S.W. Ho, and G.G. Lipscomb (eds), Ann. N.Y. Acad. Sci., 984, 142-158 (2003).

Noronha, M., Mavrov, V., and Chmiel, H., Efficient design and optimisation of two-stage NF processes by simplified process simulation, Desalination, 145, 207-215 (2002).

Prabhakar, S. and M.P.S. Ramani, A new concept of mass transfer coefficient in reverse osmosis—practical applications, J. Memb. Sci. 86 (1994) 145-154.

Pradanos, P., de Abajo, J., de la Campa, J.G., and Hernandez, A., A comparative analysis of flux limit models for ultrafiltration membranes, J. Memb. Sci., 108, 129-142 (1995).

Schaep, J., Vandecasteele, C., Mohammad, A.W., and Bowen, W.R., Analysis of the salt retention of nanofiltration membranes using the donnan-steric partitioning pore model, Sep. Sci. Tech., 34, 3009-3030 (1999).

Sirkar, K.K., Dang, P.T., and Rao, G.H., Approximate design equations for reverse osmosis desalination by spiral-wound modules, Ind. Eng. Chem. Proc. Des. Dev., 21, 517-527 (1982).

Sirkar, K.K. and Rao, G.H., Short cut design methods for reverse osmosis separation with tubular modules, Desalination, 48, 25-42 (1983).

Song, L., Flux decline in crossflow microfiltration and ultrafiltration: mechanisms and modeling of membrane fouling, J. Memb. Sci. 139 (1998) 183-200.

Song, L., J.Y. Hu, S.L. Ong, W.J. Ng, M. Elimelech, and M. Wilf, Performance limitation of the full-scale reverse osmosis process, J. of Memb. Sci. 214 (2003) 239– 244.

Sourirajan, S. and Matsuura, T., Reverse osmosis and ultrafiltration, Chap. 25 in *Encyclopedia of Fluid Mechanics*, Gulf Publishing Co., Houston, TX (1986).

Spiegler, K.S. and Kedem, O., Thermodynamics of hyperfiltration (reverse osmosis): criteria for efficient membranes, Desalination, 1, 311-326 (1966).

Thiel, S.W., Concentration-dependent solute activity coefficients and solute transport in pressure-driven membrane separation processes, J. Memb. Sci., 48, 127-140 (1990).

Wiley, D.E., Fell, C.J.D., and Fane, A.G., Optimisation of membrane module design for brackish water desalination, Desalination, 52, 249-265 (1985).

Zhenhua, H., Equations for checking flow rate parameters of a reverse osmosis device, Water Treatment, 10 (1995) 27-30.